Journal of Vertebrate Paleontology e970688 (22 pages)

DOI: 10.1080/02724634.2015.970688

ARTICLE

NEW EARLY MIOCENE PROTOCERATIDS (MAMMALIA, ARTIODACTYLA) FROM PANAMA

ALDO F. RINCON,*[,1,2] JONATHAN I. BLOCH,[1] BRUCE J. MACFADDEN,[1] and CARLOS A. JARAMILLO[3]
[1]Florida Museum of Natural History, University of Florida, Gainesville, Florida 32611, U.S.A., arincon@ufl.edu; jbloch@flmnh.ufl.edu; bmacfadd@flmnh.ufl.edu;
[2]Department of Geological Sciences, University of Florida, 241 Williamson Hall, Gainesville, Florida 32611, U.S.A.;
[3]Smithsonian Tropical Research Institute, Box 0843-03092 No. 8232, Balboa-Ancon, Panama, jaramilloc@si.edu

ABSTRACT—Although Cenozoic protoceratid artiodactyls are known from throughout North America, species referred to the Miocene protoceratine *Paratoceras* are restricted to subtropical areas of the Gulf Coast and southern Mexico and tropical areas of Panama. Newly discovered fossils from the late Arikareean Lirio Norte Local Fauna, Panama Canal basin, include partial dentitions of a protoceratid remarkably similar to those of *Paratoceras tedfordi* from Mexico, suggesting a rapid early Miocene colonization of recently emerged tropical volcanic terrains (Las Cascadas Formation). Partial lower dentitions from the overlying shallow marine to transitional Culebra Formation (early Centenario Fauna) are here referred to *Paratoceras orarius*, sp. nov., based on relatively small size, shallow mandible anterior to p3, and narrow cheek teeth. New early Hemingfordian protoceratine fossils from the upper part of the Cucaracha Formation (late Centenario Fauna) include a partial male skull and several dentitions that, together with specimens previously referred to *P. wardi* (only known from the Barstovian of Texas), are here referred to *Paratoceras coatesi*, sp. nov., based on distinctly more gracile cranial ornamentation, relatively longer nasals, a smaller and wider lower p4 (relative to m1), and more bulbous lower premolars. Results from a cladistic analysis of 15 craniodental characters coded for 11 protoceratine species suggests that *Paratoceras* is a monophyletic clade with its origin in subtropical areas of Central America, spreading into the tropics of Panama during the early Miocene (Arikareean through Hemingfordian North American Land Mammal Ages [NALMAs]), and later inhabiting subtropical areas of the Gulf Coast during the middle–late Miocene (Barstovian through Clarendonian NALMAs).

SUPPLEMENTAL DATA—Supplemental materials are available for this article for free at www.tandfonline.com/UJVP

http://zoobank.org/urn:lsid:zoobank.org:pub:31FFF397-6362-443C-A612-E9279FF122

INTRODUCTION

The Protoceratidae are characterized by an unusual cranial morphology among artiodactyls that includes the evolution of rostral cranial appendages (ossicones). The origin and evolution of the group has been the subject of debate since the establishment of the family by O. C. Marsh in 1891 when he described *Protoceras celer* Marsh, 1891, from the late Oligocene of North America. Protoceratids first appear in the North American fossil record during the late Eocene and persisted in subtropical areas until the late Miocene (Prothero, 1998). Although hypertragulid and pecoran affinities (e.g., Matthew, 1905; Frick, 1937; Scott, 1940; Stirton, 1944; Simpson, 1945; Gazin, 1955) were initially proposed, hypothetical tylopod affinities were subsequently suggested based on similarities in the structure of the pes in the late Eocene hornless protoceratids and other more derived forms (Gazin, 1955; Stirton, 1967; Patton and Taylor, 1973; Wilson, 1974; Webb and Taylor, 1980). These shared morphological similarities provided evidence for the idea that Camelidae was the sister group to Protoceratidae (including the primitive leptotragulines), with both groups the products of a late Eocene North American radiation of selenodont artiodactyls (Black, 1978; Webb and Taylor, 1980). However, later comparative work focused on basicranial morphology argued that protoceratids lacked obvious synapomorphies shared with Camelidae and highlighted the need for a systematic revision of North American Neogene fossil artiodactyls with cranial appendages (Joeckel and Stavas, 1996).

By the late Oligocene, male protoceratids exhibit a variety of cranial appendages that are unique among North American artiodactyls (Marsh, 1897; Prothero, 1998). Based on the morphology of these appendages and their associated dentitions, Frick (1937) initially proposed three Neogene subfamilies within his hypertragulid family Protoceratidae: (1) Synthetoceratinae, including the more hypsodont forms; (2) a monospecific Syndyoceratinae; and (3) Protoceratinae, including species referred to *Paratoceras* Frick, 1937, and *Protoceras* Marsh, 1891 (including the female skull of *Calops* Marsh, 1894). In a comprehensive taxonomic revision of the group, Patton and Taylor (1973) classified the non-synthetoceratine protoceratids within Protoceratinae based on fossils from the Great Plains and Gulf Coast, but excluded those primitive forms previously linked to Hypertragulidae and Camelidae. A subsequent revision of the Protoceratidae (Prothero, 1998) incorporated the tylopod relationships proposed by Black (1978) and Webb and Taylor (1980) and included the late Eocene–early Oligocene basal members proposed by Gazin (1955), Wilson (1974), and Emry and Storer (1981). Consequently, three ranks within Protoceratidae were proposed: (1) the hornless or basal protoceratids; (2) the monophyletic Synthetoceratinae of Webb, 1981; and (3) the informal 'Protoceratinae' sensu Prothero (1998).

The primitive Eocene–Oligocene hornless protoceratids inhabited a wide geographic range throughout North America, including the Great Plains and the Gulf Coast (Gazin, 1955; Wilson, 1974). They include *Leptotragulus* Scott and Osborn, 1887, from the Uintan through the Chadronian North American Land Mammal Ages (NALMAs) in Wyoming, Montana, South Dakota, Nebraska, and Utah; *Leptoreodon* Wortman, 1898, from the Duchesnean NALMA of Saskatchewan and the Uintan

*Corresponding author.

of California, Texas, and Utah; *Poabromylus* Peterson, 1931, from the Duchesnean of Utah, California, and Texas and the Chadronian NALMA of Wyoming and South Dakota; *Toromeryx* Wilson, 1974, from the Uintan of Texas; and *Heteromeryx* Matthew, 1905, from the Uintan of Texas and the Chadronian of South Dakota and Nebraska (Prothero, 1998). The monophyletic Synthetoceratinae is known from early to late Miocene (Arikareean to Clarendonian NALMAs) deposits of Wyoming, Nebraska, and the Gulf Coast (Maglio, 1966; Stirton, 1967; Patton, 1969; Patton and Taylor, 1971; Albright, 1998, 1999) and from subtropical late Miocene (Hemphillian NALMA) deposits in the Texas Gulf Coast (Patton, 1969; Webb, 1981). Synthetoceratines are characterized by their subhypsodont dentitions, relatively reduced premolars, elongate muzzles with a distinctively enlarged rostral ossicone formed by a fusion of the maxillary ossicones, and elevated postorbital ossicones in males (Patton and Taylor, 1971; Webb, 1981). The late Arikareean *Syndyoceras* Barbour, 1905 (Tribe Kyptoceratini), from Nebraska has brachydont dentitions and is the oldest member of the subfamily. On the other hand, *Prosynthetoceras* Frick, 1937, was the first synthetoceratine (Tribe Synthetoceratini) reported outside of the Great Plains, reaching areas of the Gulf Coast and New Jersey during the Arikareean, Hemingfordian, Barstovian, and Clarendonian NALMAs (Patton and Taylor, 1971; Albright, 1999).

The informal subfamily 'Protoceratinae' of Prothero (1998) (Fig. 1) includes the hornless *Pseudoprotoceras* Cook, 1934, from the Chadronian and Orellan NALMAs of Wyoming, Nebraska, and Saskatchewan (Emry and Storer, 1981); *Protoceras* from the Whitneyan and Arikareean of South Dakota, Nebraska, Wyoming, and Texas (Patton and Taylor, 1973; Albright, 1999); and the more tropical *Paratoceras* Frick, 1937, from the Arikareean, Barstovian, and Clarendonian deposits of Mexico, Texas, and the Hemingfordian of Panama (Whitmore and Stewart, 1965; Patton, 1969; Patton and Taylor, 1973; Webb et al., 2003; Kirby and MacFadden, 2005; MacFadden, 2006).

Early Miocene protoceratids are rare in the relatively well-sampled fossiliferous sequences of the Great Plains and are represented only by the late Arikareean protoceratine *Protoceras neatodelpha* Patton and Taylor, 1973, and the Hemingfordian synthetoceratine *Lambdoceras* Stirton, 1967. During the Neogene, synthetoceratines were not only the dominant protoceratids in subtropical fossil assemblages of the Gulf Coast (Patton, 1969; Patton and Taylor, 1973; Albright, 1999), but also reached temperate areas of the Atlantic Coastal Plain (Tedford and Hunter, 1984). On the other hand, the more tropical protoceratines inhabited Panama (Whitmore and Stewart, 1965; MacFadden, 2006) and Mexico (Webb et al., 2003) and are documented from at least one occurrence of *Paratoceras wardi* in Barstovian deposits of Texas. Surprisingly, *Paratoceras* is not reported from any of the other well-sampled units that constitute the Coastal Plain, yet it is reported from Miocene fossil assemblages in Mexico and Panama (Patton and Taylor, 1973; MacFadden, 2006). By the middle to late Miocene, protoceratids became increasingly rare in the Great Plains. The protoceratine *Paratoceras* persisted in the Gulf Coast (Texas), whereas the synthetoceratine *Kyptoceras* persisted in Mexico and the Atlantic Coastal Plain

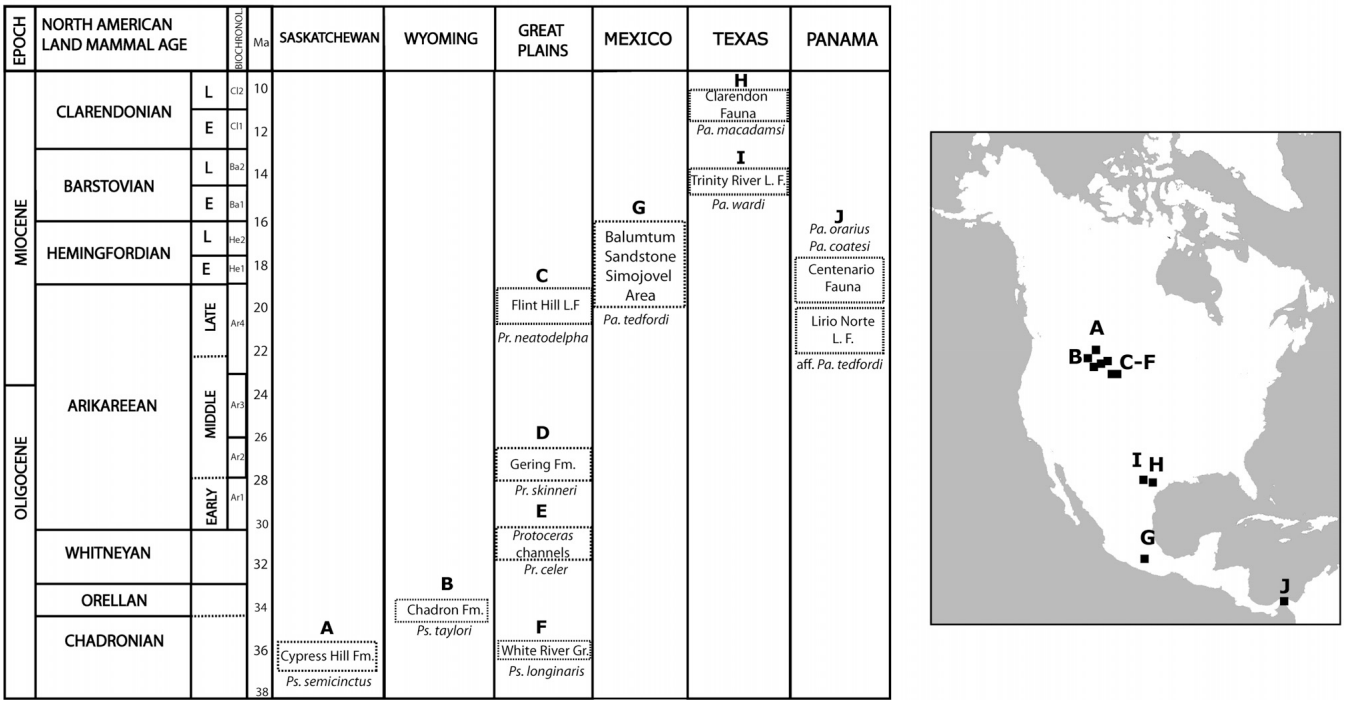

FIGURE 1. Location and biochronology of the protoceratine-bearing fossil faunas discussed in this study. **A**, *Pseudoprotoceras semicinctus* from the Chadronian Cypress Hill Formation in Saskatchewan, Canada, and the White River Formation of Wyoming (Emry and Storer, 1981); **B**, *Pseudoprotoceras taylori* from the late Chadronian White River Formation in Wyoming (Emry and Storer, 1981); **C**, *Protoceras neatodelpha* from the late Arikareean of Niobrara County, Wyoming (Patton and Taylor, 1973); **D**, *Protoceras skinneri* from the Gering Formation (early Arikareean) of South Dakota and Nebraska; **E**, *Protoceras celer* from the Whitneyan Protoceras channels, White River, South Dakota (Patton and Taylor, 1973); **F**, *Pseudoprotoceras longinaris* from the Chadronian of Wyoming and Nebraska (Cook, 1934); **G**, *Paratoceras tedfordi* from the late Oligocene–early Miocene Balumtum Sandstone in the Simojovel area, southern Mexico (Webb et al., 2003); **H**, *Paratoceras wardi* from the Barstovian Trinity River L. F. in Texas (Patton and Taylor, 1973); **I**, *Paratoceras macadamsi* from the Clarendonian Clarendon Fauna of Texas (Patton and Taylor, 1973); **J**, *Paratoceras* spp. (this study) from the late Arikareean Lirio Norte L. F. and the Hemingfordian Centenario Fauna from the Panama Canal Area (Rincon et al., 2012a, 2012b; 2013; MacFadden et al., 2010). Chronostratigraphy and biochronology modified from Albright et al. (2008). **Abbreviations**: **Ar**, Arikareean Faunal Zone; **Ba**, Barstovian Faunal Zone; **Cl**, Clarendonian Faunal Zone; **E**, early; **He**, Hemingfordian Faunal Zone; **L**, late; **L. F.**, Local Fauna; **Pa.**, *Paratoceras*; **Pr.**, *Protoceras*; **Ps.**, *Pseudoprotoceras*.

until the early Pliocene (Hemphillian NALMA) (Patton and Taylor, 1973; Webb et al., 2003). This, along with the more common occurrence of protoceratines in the Miocene fossil record of Texas and Central America, suggests that protoceratines could have diversified in the poorly sampled tropical areas of Central America during the Miocene prior to their last occurrence in late Miocene deposits from Texas (Patton and Taylor, 1973; Webb, 1981). Although synthetoceratines probably persisted as tropical browsers in the Gulf Coast and the Atlantic Coastal Plain, the observed increase in crown height in Synthetoceratini and Kyptoceratini has been interpreted to be associated with a gradual shift towards a coarser feeding capacity during increasing dry seasons throughout the Neogene (Webb et al., 2003).

An early Miocene diversification of protoceratines would have been contemporaneous with floristic changes documented in the fossil record of the Great Plains, where a gradual replacement of woodland savannas by grass-dominated habitats has been recognized on the basis of the relative abundance of palynomorphs (Strömberg, 2002, 2006). It has been suggested that these changes in paleoecology are associated with changes in species richness and generic diversity of ungulate browser communities during the early–middle Miocene in the Great Plains (Janis et al., 2000; Woodburne, 2004).

The purpose of this paper is to describe new early Miocene protoceratid fossils recently collected from three different lithostratigraphic units (Las Cascadas, Culebra, and Cucaracha formations) cropping out along the Gaillard Cut in the Panama Canal area (Fig. 2) and reevaluate specimens (casts) originally reported by Whitmore and Stewart (1965) and further investigated by MacFadden (2006). In order to clarify the systematic taxonomy and improve the poorly known paleobiogeography of these Central America protoceratines, we compare the new Panamanian fossils with Neogene protoceratines from more temperate sequences of the Great Plains, the Texas Gulf Coast (Patton and Taylor, 1973), and Mexico (Webb et al., 2003) in a phylogenetic context. The resulting systematic, paleogeographic, and biostratigraphic implications are discussed while also incorporating paleobotanical evidence regarding the early Miocene tropical forest of Panama and southern Mexico.

Early Miocene Mammals from Panama—The early Miocene (~25–19 Ma) volcaniclastic sequences (Kirby et al., 2008; Farris et al., 2011; Montes et al., 2012) cropping out along the Gaillard Cut area (Fig. 2) include a succession of mammalian faunas unsurpassed anywhere in Central America and provide the basis for faunal and paleoecological comparisons between tropical areas of southern Central America and more temperate areas of North America (e.g., Great Plains and the Gulf Coast). The early Miocene terrestrial mammalian communities from the Gaillard Cut have exclusively North American affinities (Whitmore and Stewart, 1965; MacFadden, 2006; Rincon et al., 2012b). They inhabited tropical southern Central America prior to the final closure of the Central American Seaway approximately 3–4 Ma (Woodburne, 2010).

Among those fossil mammals initially reported by Whitmore and Stewart (1965) from the Cucaracha Formation, a collection of brachydont artiodactyl dentitions were assigned to Protoceratidae based on their resemblance to *Protoceras* (Whitmore and Stewart, 1965). Although the taxonomy of protoceratines is largely based on the morphology of the skull, previous studies were limited to these fragmentary dentitions. Analysis of the dental dimensions of the Panamanian protoceratids concluded that they were 12% larger than those of *Paratoceras wardi* Patton and Tylor, 1973, from the Barstovian from Texas (Kirby and MacFadden, 2005), and these brachydont dentitions were subsequently attributed to *P. wardi* after direct comparison of these collections with the topotypic hypodigm of this taxon from the Barstovian Trinity River Local Fauna (L. F.) in Texas (MacFadden, 2006).

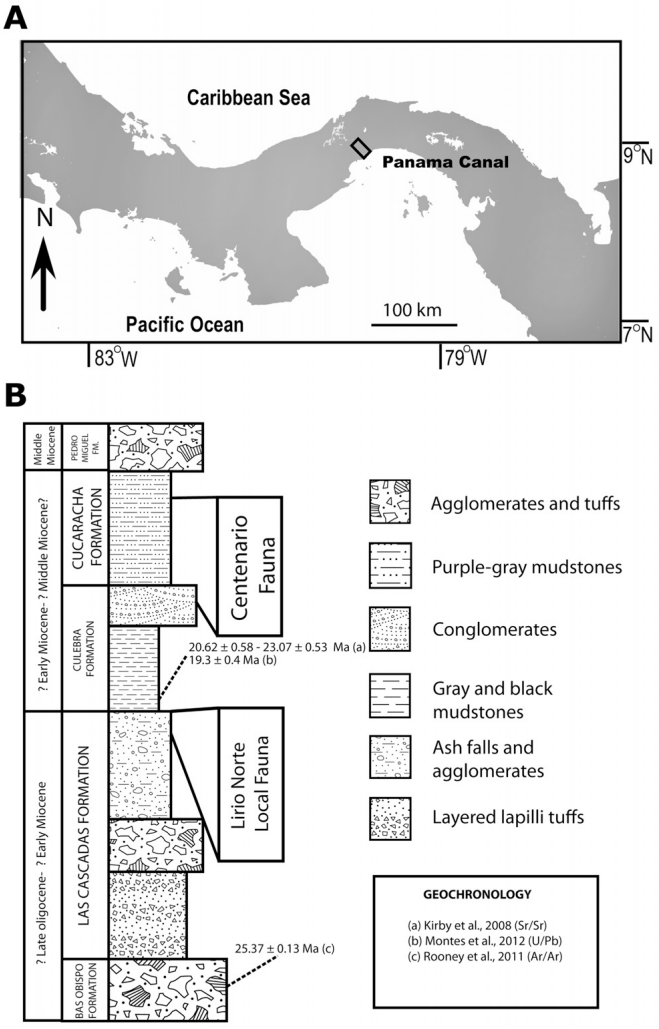

FIGURE 2. Location and stratigraphic position of protoceratine fossils from the Gaillard Cut, Panama Canal area. **A**, map of North and Central America showing the location of the Panama Canal area and the Gaillard Cut; **B**, schematic stratigraphic section of the Gaillard Cut area showing the stratigraphic position of the Lirio Norte Local Fauna (L. F.) and the Centenario Fauna. Modified from Rincon et al., 2013. After Kirby et al., 2008; Rooney et al., 2010; Montes et al., 2012; Rincon et al., 2012a.

Early Miocene Paleoecology of Southern Central America—Despite the abundance of protoceratids in the early Miocene fossil record of the Gulf Coast, and southern Central America, protoceratine paleocology is limited to inferences based on their postcranial and dental morphology (Prothero, 1998), with only a few isotopic analyses carried out on fossil dentitions from Panama (MacFadden and Higgins, 2004). Bulk carbon isotopic values measured on tooth enamel of *Paratoceras* from the late Centenario Fauna, (mean value of −11.3‰) were consistent with a specialized diet of xeric adapted C3 browse or possibly a minor (<20%) dietary component of C4 plants (MacFadden and Higgins, 2004; MacFadden et al., 2014).

Additional paleoecological evidence regarding the floral composition of forested areas of southern Central America can be compiled from palynological and paleobotanical studies of the late Oligocene–early Miocene fossil record of southern Mexico and Panama. In southern Mexico, the La Quinta Flora includes fossiliferous late Oligocene–early Miocene amber-bearing sequences underlying the Balumtum Sandstone, where the

protoceratine *Paratoceras tedfordi* was recovered (Graham, 1999a; Webb et al., 2003) (Fig. 1). The assemblage includes palynomorphs that are representative of ecosystems ranging from mangrove swamps to lowland riparian forests, tropical rain forests, lower montane environments, and evergreen and tropical deciduous forests (Graham, 1999a). By the early and middle Miocene, presence of more temperate taxa in the Mendez palynoflora of northern Chiapas (Graham, 1999b) and the middle to late Miocene Ixtapa palynoflora indicate elements of more temperate vegetation, with presence of higher-elevation taxa preserved in estuarine and transitional environments (Graham, 1985, 1999a, 1999b).

These phytogeographic patterns are remarkably different in tropical areas of southern Central America. Early Miocene palynofloras from central Panama (Panama Canal area) are dominated by tropical rainforest and lower montane to montane forest with a low proportion (~10%) of North American Laurasian taxa (Graham, 1988a, 1988b; Jaramillo et al., 2014). These tropical floral affinities have also been identified in the older paleobotanical records from western Panama, where permineralized endocarps and seeds suggest that families typical of extant tropical rainforest colonized ancient volcanic terrains of Panama in the Eocene (Herrera et al., 2012).

Biochronology and Dental Nomenclature—The biochronology follows the late Oligocene–early Miocene biozonation developed by Tedford et al. (2004) and the subsequent recalibration proposed by Albright et al. (2008) for the Arikareean North America Land Mammal Age (NALMA). For the most part, dental nomenclature follows Patton and Taylor (1973:fig. 2). We also use the descriptive system of crests and crescents defined by Loomis (1925) for selenodont dentitions in artiodactyls.

Institutional Abbreviations—**AMNH F:AM**, Frick: American Mammals collection at the American Museum of Natural History, New York, U.S.A; **UCMP**, University of California Museum of Paleontology, Berkeley, California, U.S.A; **UF**, vertebrate paleontology collection, Florida Museum of Natural History (FLMNH), University of Florida, Gainesville, Florida, U.S.A; **UNSM**, University of Nebraska State Museum, Lincoln, Nebraska, U.S.A.

Other Abbreviations—**APL**, anterior-posterior length (in millimeters); **TW**, transverse width (in millimeters).

GEOLOGIC SETTING AND BIOCHRONOLOGY

The late Oligocene and early Miocene lithostratigraphic units cropping out along the Panama Canal (Fig. 2) represent a succession of subaerial volcanic and volcanoclastic sequences (Bas Obispo and Las Cascadas formations) underlying the shallow marine, transitional, and continental sequences of the Culebra and Cucaracha formations (Kirby et al., 2008; Rooney et al., 2010; Montes et al., 2012). The volcanic and volcaniclastic Pedro Miguel Formation followed the accumulation of the continental paleosols of the upper part of the Cucaracha Formation and represents the youngest formal lithostratigraphic unit in the Gaillard Cut area (Fig. 2).

The early Miocene Las Cascadas Formation represents the oldest fossiliferous continental sequence cropping out along the Panama Canal area (Montes et al., 2012; Rincon et al., 2012a) (Fig. 2). The basal part, mostly non-fossiliferous layered lapilli tuffs, unconformably overlies the welded and massive volcanic agglomerates of the middle to late Oligocene Bas Obispo Formation (Woodring and Thompson, 1949; Woodring, 1957, 1982; Farris et al., 2011; Montes et al., 2012). The upper part is characterized by fossiliferous volcaniclastic sequences deposited in alluvial depositional settings and sparse fossiliferous coarser volcanic agglomerates and conglomeratic sequences (Montes et al., 2012). The stratigraphic relationships of these fossil vertebrates (overlying the agglomerates of the Bas Obispo and the fine-grained tuffaceous lower Las Cascadas Formation) (Fig. 2) indicate that the fossil assemblage represents the arrival of northern populations into a recently emerged continental area connected with subtropical North American continental terrains (Rincon et al., 2012a, 2012b, 2013). The occurrence of the European amphicyonid *Cynelos* Jourdan, 1862, and the inferred ages for the floridatraguline camels place this fossil assemblage in the late Arikareean (Ar4) NALMA (Tedford et al., 2004; Rincon et al., 2012a, 2012b).

The fossil mammals initially reported by Whitmore and Stewart (1965) were described and included into the Gaillard Cut Local Fauna (MacFadden, 2006, and references therein). Based on the stratigraphic distribution of the fossil tayassuids, spanning about ~115 m along the Culebra and Cucaracha formations, these mammalian fossils provided the basis for the Centenario Fauna (MacFadden et al., 2010). The Centenario Fauna includes a complex mixture of early Miocene taxa that taken together indicate an early Hemingfordian (He1) NALMA (MacFadden et al., 2014).

The fossil protoceratids described here as part of the Centenario Fauna were collected from two different lithostratigraphic levels (Fig. 2): the fossiliferous conglomerates of the upper part of the Culebra Formation, which were deposited in deltaic fluvial channels with transitional to shallow marine influence (Kirby et al., 2008; MacFadden et al., 2010; Montes et al., 2012), and the more continental sequences of the upper part of the Cucaracha Formation (Retallack and Kirby, 2007; Kirby et al., 2008). Although the Centenario Fauna includes a number of localities with similar stratigraphic ranges along the Gaillard Cut area (MacFadden et al., 2010), the late Arikareean Las Cascadas fossil assemblage spans an approximately 15 m fossiliferous sequence that is restricted to a single locality in the uppermost Las Cascadas Formation in the Lirio Norte area (Rincon et al., 2012a, 2012b, 2013). The fauna represented by these associated early Miocene vertebrates within this limited geographic and stratigraphic distribution are herein referred to as the Lirio Norte Local Fauna (L. F.) (Fig. 2) following the principles and biostratigraphic nomenclature proposed by Tedford (1970).

SYSTEMATIC PALEONTOLOGY

Class MAMMALIA Linnaeus, 1758
Order ARTIODACTYLA Owen, 1848
Suborder TYLOPODA Illiger, 1811
Family PROTOCERATIDAE Marsh, 1891
Subfamily PROTOCERATINAE Marsh, 1891
Genus *PARATOCERAS* Frick, 1937

Type Species—*Paratoceras macadamsi* Frick, 1937, from the Clarendonian Clarendon Fauna, Texas.

Type Specimen—AMNH F:AM 32457, right partial mandible with p2–m3 (broken).

Included Species—*Paratoceras tedfordi* Webb et al., 2003, from the early Miocene Balumtum Sandstone from the Simojovel area in the state of Chiapas, Mexico; *P. wardi* Patton and Taylor, 1973, from the Barstovian Trinity River Local Fauna (L. F.) in San Jacinto and Walker counties, Texas; *P.* aff. *tedfordi* from the late Arikareean Lirio Norte L. F. in Panama; *P. orarius*, sp. nov., from the early Centenario Fauna (Upper Culebra Formation) in Panama; and *P. coatesi*, sp. nov., from the late Centenario Fauna (Upper Cucaracha Formation) in Panama (Figs. 1, 2).

Comments—Frick (1937) provided the original generic description based on a partial lower dentition with Rp2–m3 (AMNH F:AM 32457) of the Clarendonian *P. macadamsi* Frick, 1937, from the MacAdams Ranch Quarry, Donley County, Texas (Frick, 1937:608). Based on an exceptionally well-preserved male

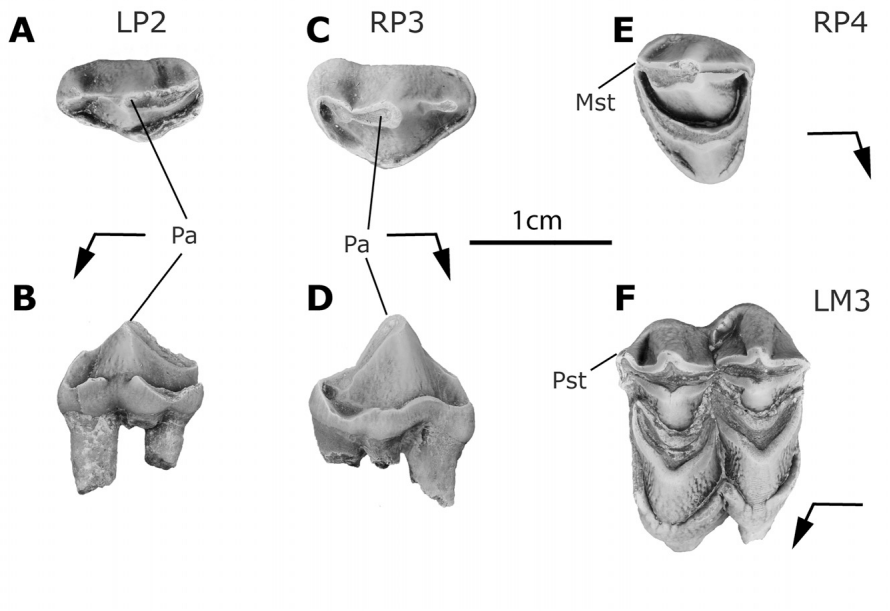

FIGURE 3. Upper dentition of *Paratoceras* aff. *P tedfordi* from the late Arikareean Lirio Norte L. F. **A**, UF 244199, left P2, occlusal view; **B**, UF 244199, lingual view; **C**, UF 271626, right P3, occlusal view; **D**, UF 271626, right P3, lingual view; **E**, UF 271618, right P4, occlusal view; **F**, UF 236931, left M2, occlusal view. **Abbreviations**: **Mst**, Metastyle; **Pa**, Paracone; **Pst**, Parastyle. Arrows point anterolingually.

skull and several partial dentitions, Patton and Taylor (1973) presented a revised diagnosis for the genus and discussed its relationships with other protoceratines after describing a new species (*P. wardi* Patton and Taylor, 1973) from the early Barstovian Fleming Formation, San Jacinto County, Texas (Tedford et al., 2004). Because even partial skulls of *Paratoceras* are relatively rare in the fossil record, we compile the cranial and dental morphologies described by Patton and Taylor (1973) and later summarized by Prothero (1998).

The male skull of *Paratoceras* is characterized by the absence of parietal protuberances, presence of weak parietal ridges, a faint sagittal crest, and a distinct transversely forked occipital horn (Patton and Taylor, 1973:fig. 5). *Paratoceras* further differs from *Protoceras* in having smaller (relative to skull length) and more posteriorly located maxillary protuberances (relative to the position of the anterior root of P2); the supraorbital ossicones are taller (relative to their length), more gently recurved, and have distinctive flared and triangular basal segments and bulbous tips (Patton and Taylor, 1973:fig. 5). The orbits of *Paratoceras* are more anteriorly placed relative to the posterior root of M3, the facial region is shorter (relative to the skull length), and the premolars are shorter (relative to M1 or m1; APL) and more bulbous than those of *Protoceras*. The crowns of the molars are higher relative to length, and the lingual cinguli on P2–P3 are more reduced. The protocone on P3 is reduced in all dimensions compared with the other cusps and often represented exclusively by a small cuspule connected to the cingulum.

Paratoceras differs from *Pseudoprotoceras* in being larger, having maxillary and frontal protuberances on the male skull, having a narrow (relative to APL) P2 with no lingual cingulum and a reduced number of cusps, and upper molars with continuous lingual cingula. The lower premolars of *Paratoceras* have paraconids that are not anterolingually directed and lack the distinct anterolingually inflected metaconids of *Pseudoprotoceras* (Emry and Storer, 1981).

Paratoceras tedfordi, the oldest member of the genus, was found in amber deposits of the late Oligocene–early Miocene Balumtum Sandstone (22–26 Ma) in southern Mexico (Webb et al., 2003). Recently published Sr/Sr dates (ca. 20–23 Ma) for the underlying Mazantic Shale and the Mucuzpana Limestone (Vega et al., 2009) coupled with biostratigraphy of benthic and planktonic foraminifera (Solórzano-Kraemer, 2007, 2010) suggest a younger age (early Miocene) for the amber-bearing sequences. Unfortunately, the stratigraphic relationships of the main fossil-bearing units in the Simojovel area are still unclear (Solórzano-Kraemer, 2010).

PARATOCERAS aff. *P. TEDFORDI*
(Figs. 3, 4; Table 1)

Locality and Horizon—Lirio Norte L. F. (site YPA-024 in UF Vertebrate Paleontology Collection), Panama Canal area, Panama, Central America. Fossils were collected in the upper part of the Las Cascadas Formation (Fig. 2), equivalent to the late Arikareean Ar4 NALMA (Fig. 1) (Rincon et al., 2012a, 2012b).

Referred Material—UF 244199, left P2; UF 271626, right P3; UF 271618, right P4; UF 271620, left M2; UF 236931, left M2; UF 275168, left mandible with Lm2–m3; UF 267194, right mandible with Rp4–m3; UF 254119, right p4; UF 244213, right m1; UF 271627, right m2; UF 254121, left m2; UF 271179, left m2; UF 271622, left m2.

Description

Upper Dentition—The P2 (Fig. 3A, B) is tri-rooted, with the lingual root located close to the posterolabial root. The crown is elongate (APL > TW), lacks external ribs, and has a distinct paracone interrupting an internal cingulum that widens posteriorly and which encloses a small open basin lingual to the metastyle. The parastyle, paracone, and metastyle are aligned, forming a straight labial margin. The anterolingual crescent is low and formed by a not very distinct small cingular segment. The posterolingual crescent is also low and formed by a distinct small cingular segment that extends lingually from the base of the paracone towards the posterior margin, but which never reaches the lingual part of the base of the metastyle.

The P3 (Fig. 3C, D) is also tri-rooted, but with a more lingually expanded crown at its midpoint (forming a more distinct 'wedge shape') than that of P2. The crown of P3 further differs from that of P2 in having a distinctively higher and stronger

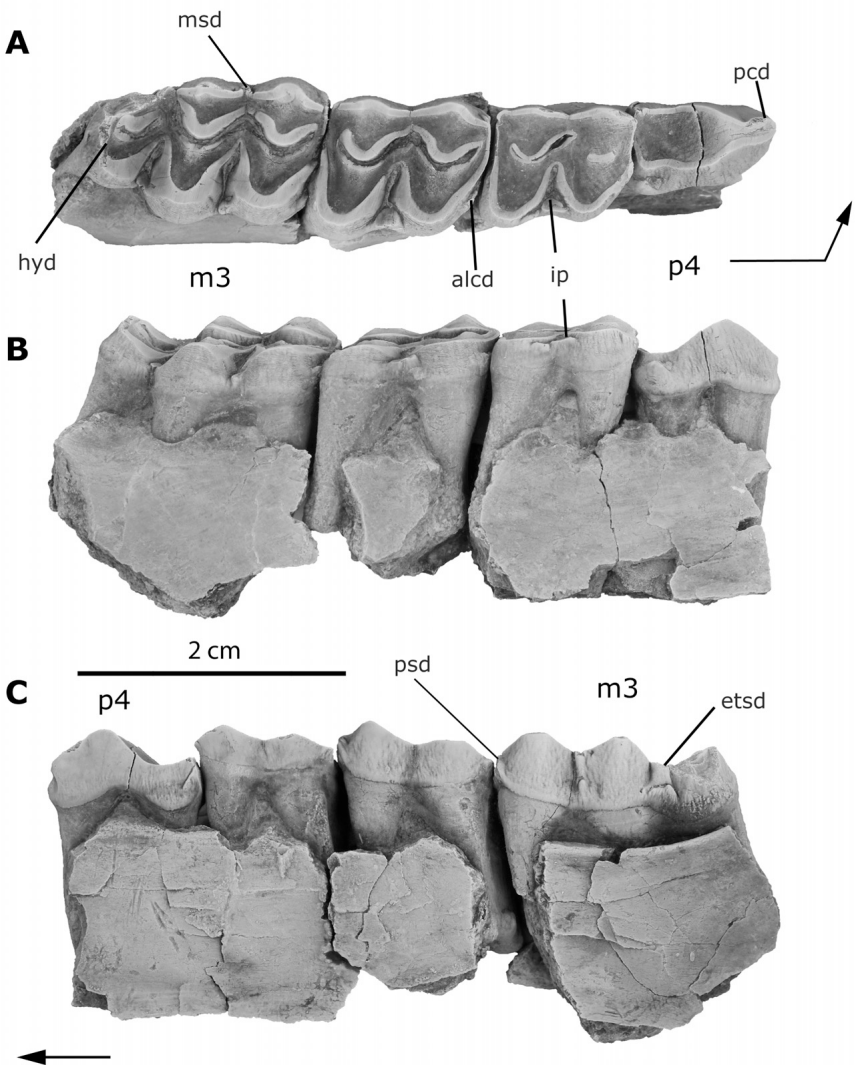

FIGURE 4. Lower dentition of *Paratoceras* aff. *P. tedfordi* from the Lirio Norte L. F. UF 267194, partial left mandible with p4–m3. **A**, occlusal view; **B**, labial view; **C**, lingual view. **Abbreviations**: **alcd**, anterolingual cingulid; **etsd**, entostylid; **hyd**, hypoconid; **ip**, intercolumnar pillar; **msd**, metastylid; **psd**, parastylid. Arrows point anterolingually.

TABLE 1. Summary table of dental measurements (in mm) of *Paratoceras* aff. *P. tedfordi* from the Las Cascadas Formation.

Tooth position (Dimension)	N	Range	Mean	Standard deviation	Coefficient of variation
			Lower molars		
p4 (APL)	2	10.54–11.60	11.07	0.44	3.97
p4 (TW)	2	6.50–7.01	6.76	0.36	5.32
m1 (APL)	1	10.55	10.55	—	—
m1 (TW)	1	9.24	9.24	—	—
m2 (APL)	5	12.12–14.60	13.53	1.27	9.38
m2 (TW)	5	10.2–11.27	10.9	0.32	2.98
m3 (APL)	2	18.12–21.08	19.6	2.09	10.66
m3 (TW)	2	10.40–10.67	10.54	0.19	1.88
m3 (TWhyd)	2	6.56–6.85	6.70	0.20	3.05
			Upper molars		
P2 (APL)	1	10.54	10.54	—	—
P2 (TW)	1	6.01	6.01	—	—
P3 (APL)	1	10.43	10.43	—	—
P3 (TW)	1	6.11	6.11	—	—
P4 (APL)	1	8.78	8.78	—	—
P4 (TW)	1	11.01	11.01	—	—
M2 (APL)	1	13.03	13.03	—	—
M2 (TW)	1	16.68	16.68	—	—

Abbreviations: **APL**, anterior-posterior length; **TW**, transverse width; **TWhyd**, hypoconulid transverse width.

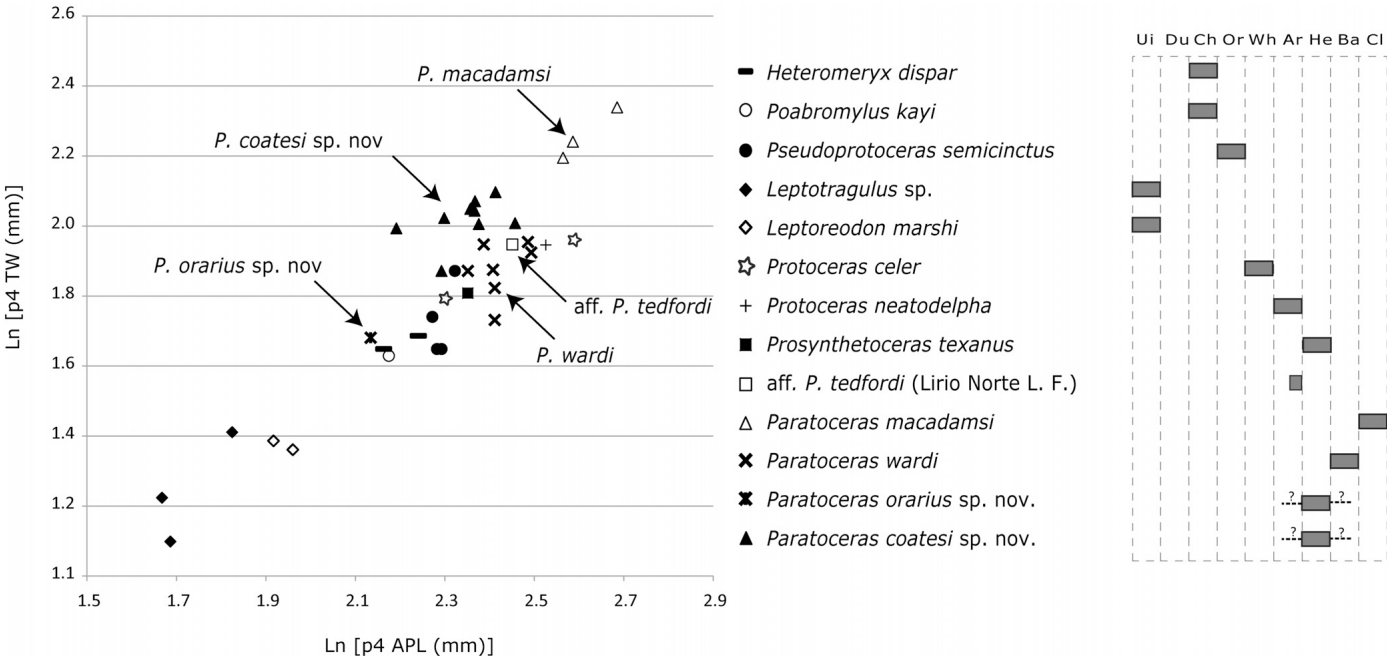

FIGURE 5. Bivariate plots of the natural logarithm of the anterior-posterior length versus maximum transverse width of the lower p4 for relevant specimens of Protoceratidae and their biostratigraphic distribution. **Abbreviations**: **APL**, anterior-posterior length; **Ar**, Arikareean Faunal Zone; **Ba**, Barstovian Faunal Zone; **Ch**, Chadronian Faunal Zone; **Cl**, Clarendonian Faunal Zone; **Du**, Duchesnean Faunal Zone; **He**, Hemingfordian Faunal Zone; **TW**, transverse width; **Ui**, Uintan Faunal Zone; **Wh**, Whitneyan Faunal Zone.

paracone, a metastyle that is less distinct and slightly recurved labially, and an internal cingulum that is more nearly continuous and reaches the labial segments of both the parastyle and the mesostyle. The internal cingulum forms a narrow valley anterior to the labial surface of the paracone (Fig. 3C, D) and a wider valley on the surface posterior to the paracone. There is no evidence of a functional protocone, with only a basal widening of the lingual cingulum present on that part of the crown. The parastyle, paracone, and metastyle are aligned, forming a straight labial margin with no labial projection of the metastyle.

The crown of P4 (Fig. 3E) is triangular (labial longer than lingual margin) and submolariform, with the development of a crescent but lacking a metacone and hypocone. Its crescent is asymmetric, with a shorter anterior crista that is responsible for an anteriorly placed protocone. The metastyle is distinct, whereas the parastyle is only evident at the basal part of the crown. The internal cingulum is weak and interrupted by the lingual part of the protocone.

The crown of M2 is wider than it is long and has thick, crenulated enamel (Fig. 3F). The parastyle is distinct, and strong ribs extend up the anterior and posterior crests from the base of the crown to the tip of both the paracone and metacone. The crests are parallel and there is no anterior overlap between them, resulting in the lack of a well-developed mesostyle, which is only partially represented by an apical extension of the basal cingular segment located labially between the crests. The shape of the crescents varies from an open (towards the labial margin) 'V' for the posterior crescent to a more closed 'V' for the anterior crescent. Crescents are asymmetric, with relatively longer anterior cristae that are responsible for a wider (relative to APL) anterior (compared with posterior) aspect of the crown. A strong continuous basal cingulum connects the anterior and posterior crests on the lingual margin of the crown and converges in an intercolumnar pillar at the labial opening of the transverse valley (Fig. 3F).

Lower Dentition—In UF 267194, the crown of p4 is elongate (APL > TW) and longer than that of m1 (Table 1). The anterior margin is formed by a narrow and abbreviated paraconid, whereas the posterior margin is fashioned by a distinctive labial cuspulid at the base of the crown (Fig. 4A). It has a high protoconid and a low and straight paraconid. The metaconid and entoconid are present on the margins of a wide talonid. The lower molars are brachydont, with deep anterior and posterior fossettids and crenulated thick enamel (Fig. 4A). Each molar has two discontinuous and overlapping crests with a distinctive metastylid. The metaconid crest is well separated from the rest of the tooth in early wear stages. The crescents are asymmetric, with long anterior cristids that are responsible for the posteriorly positioned protoconid and hypoconid. A distinctive basal cingulid is present anterior to the protoconid (Fig. 4B) and connects the base of the parastylid with the labial margin of the anterior crescent. The intercolumnar pillars are restricted to the basal part of the protoconid and hypoconid crests along the molar series (Fig. 4B). The parastylids are well developed and a strong and distinct entostylid is present on the m3 (Fig. 4C). Two enamel ridges divide the hypoconulid of m3 (Fig. 4A). The lingual ridge is broader than the labial ridge and encloses a distinct invagination restricted to the apical segment of the crown.

Discussion and Comparisons—Brachydont partial dentitions from the Lirio Norte L. F. are referred to the genus *Paratoceras* Frick, 1937, based on the presence of a distinctive posteriorly wide and wedge-shaped p4, lack of a distinctive protocone on P2 and P3, and the absence of convex labial margins in the upper premolars, the lattermost being a distinctive morphology present in *Protoceras celer* and faintly noticeable in *Protoceras skinneri* (Patton and Taylor, 1973). Although weaker than those present in *P. wardi*, the cingula on both the anterior and posterior parts of the crescents on M2 are continuous and closely resemble those of the holotype of *Paratoceras tedfordi* (Webb et al., 2003: fig. 14.3). This condition is in direct contrast to that of *Protoceras, Pseudoprotoceras*, and *Prosynthetoceras*, which have less

nearly continuous cingular segments that are more restricted to the anterior part of the crescents (Frick, 1937; Patton and Taylor, 1973; Emry and Storer, 1981). The straight paraconid and elongate p4 of *Paratoceras* from the Lirio Norte L. F. are more similar to those of *P. wardi* (Fig. 5) than those of *P. coatesi*, sp. nov., from the younger Centenario Fauna (see below). *Paratoceras* from the Lirio Norte L. F. has an approximate APLp4/APLm1 ratio of 1.10, whereas *P. wardi, P. orarius*, sp. nov., and *P. coatesi*, sp. nov., have ratios of 1.02, 0.90, and 0.87, respectively (see below). Although the distinctive strong parastylid (Fig. 4C) present on the lower molars from the Lirio Norte L. F. seems to be unique among species currently allocated to *Paratoceras*, we are reluctant to name a new species because the morphology of the upper dentition is so similar to that of *P. tedfordi*, for which the lower dentition is still unknown (Webb et al., 2003). Our designation (*Paratoceras* aff. *P. tedfordi*) is supported by the similar dimensions of the M2 (Fig. 6), the development of the protocone in P2 and P3, and shared morphologies of the cingular segments in the upper molars.

The morphology of the talonid of m3 is somewhat similar to that of floridatraguline camels recovered from the same locality (a divided hypoconulid where both the lingual and labial selenes are projections of the hypoconid and entoconid); however, protoceratines are characterized by the presence of wider lower molars with thick crenulated enamel, less reduced premolars, and a distinctive shallower invagination of the talonid of m3 that is only evident in unworn stages (Rincon et al., 2012a).

PARATOCERAS ORARIUS, sp. nov.
(Fig. 7; Table 2; Appendix 1)

P. wardi Kirby, Jones, and MacFadden (2008:6).

Holotype—UF 271625, right partial mandible with p3–m3 (Fig. 7).

Locality and Horizon—UF 271625 was found in the Lirio Sector (YPA-063 in UF Vertebrate Paleontology Collection, Panama Canal area (Fig. 1); UF 237878, UF 280224, and UF 267081 were found in similar stratigraphic levels (YPA-015, YPA-084, and YPA-016, respectively) along the upper part of the Culebra Formation (Fig. 2) in the Lirio Sector. These lithostratigraphic levels are approximately equivalent to the levels containing specimens of '*Cynorca*' *occidentale* Woodburne, 1969

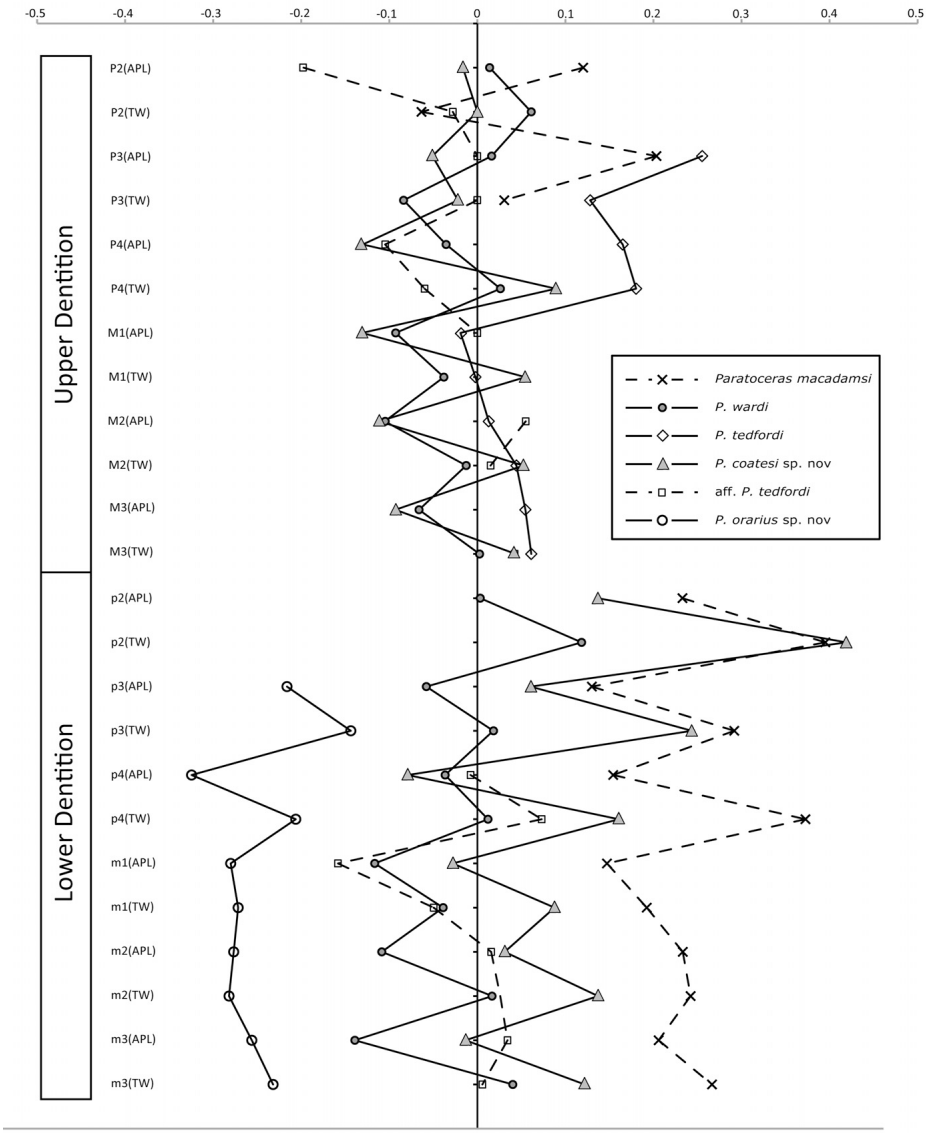

FIGURE 6. Natural log-ratio diagram for dental measurements of *Paratoceras* spp. using *Protoceras celer* as a standard for comparison (straight line at zero). **Abbreviations**: **APL**, anterior-posterior length; **TW**, transverse width.

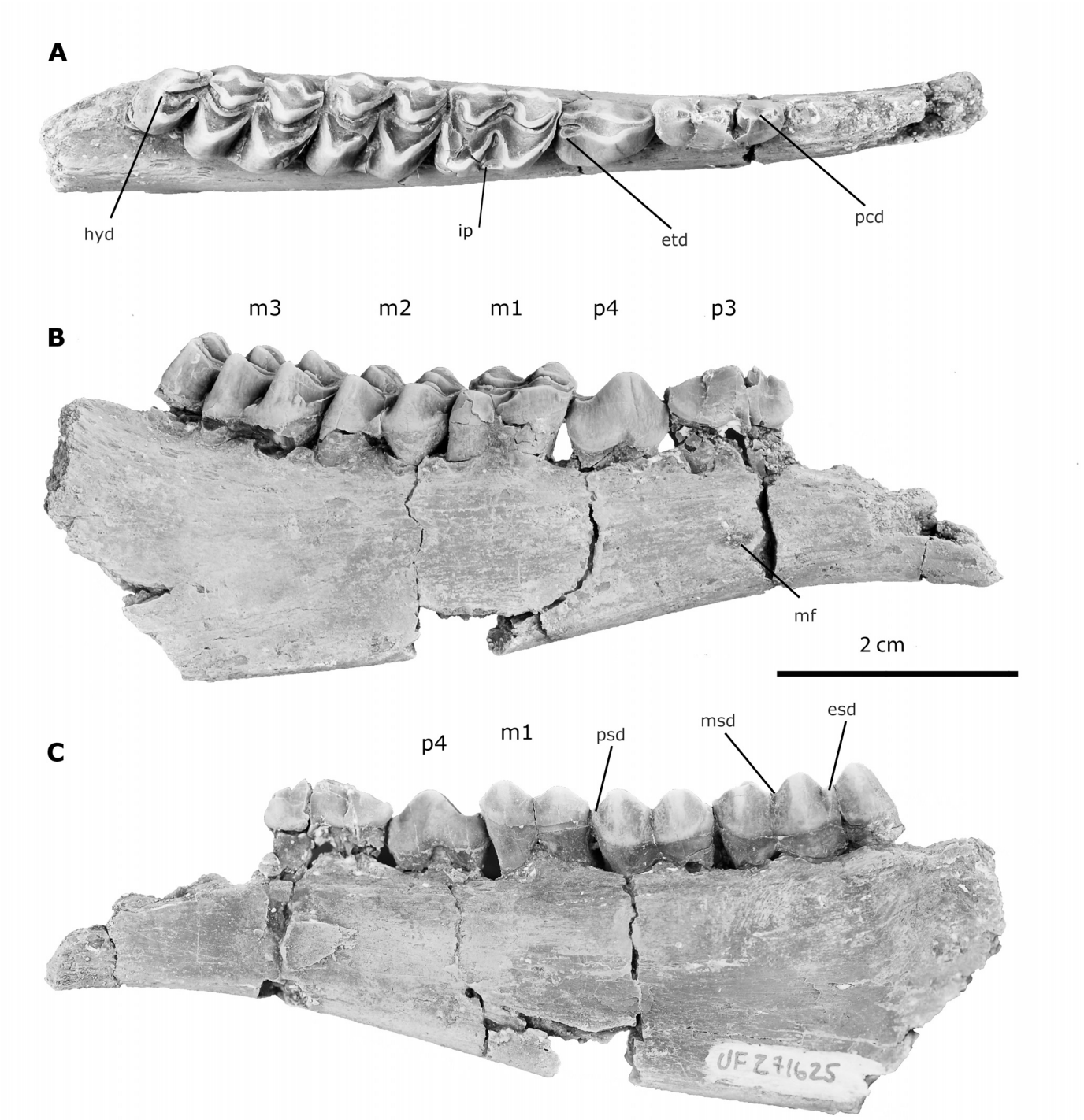

FIGURE 7. Lower dentition of *Paratoceras orarius*, sp. nov., from the upper Culebra Formation, UF 271625 (holotype), partial dentary with left p3–m3, left c1. **A**, occlusal view; **B**, labial view; **C**, lingual view. **Abbreviations**: **esd**, entostylid; **etd**, entoconid; **hyd**, hypoconid; **ip**, intercolumnar pillar; **mf**, mental foramen; **msd**, metastylid; **pcd**, paraconid; **psd**, parastylid.

(MacFadden et al., 2010:fig.2), and are correlative to Section 3 of Kirby et al., 2008:fig. 6. These intervals are interpreted to represent the early Hemingfordian NALMA (He1) based on the occurrence of the rhinocerotids *Menoceras barbouri* Troxell, 1921, and *Floridaceras whitei* Wood, 1964, also reported by MacFadden, 2006, and Kirby et al., 2008 (Tedford et al., 2004), and the independent age determinations provided by MacFadden et al. (2014).

Etymology—'Orarius' from Greek: estuarine or coastal, referring to the inferred sedimentary environment represented by the upper Culebra Formation (Retallack and Kirby, 2007), where the holotype was found.

TABLE 2. Summary table of dental measurements (in mm) of *Paratoceras orarius*, sp. nov., from the upper Culebra Formation.

Tooth position (Dimension)	N	Range	Mean	Standard deviation	Coefficient of variation
			Lower molars		
p3 (APL)	1	10.73	10.73	—	—
p3 (TW)	1	4.27	4.27	—	—
p4 (APL)	1	8.45	8.45	—	—
p4 (TW)	1	5.37	8.45	—	—
m1 (APL)	2	9.25–9.42	9.34	0.12	1.28
m1 (TW)	2	7.18–7.61	7.40	0.304	4.10
m2 (APL)	3	9.84–10.42	10.10	0.293	2.90
m2 (TW)	3	7.62–8.40	8.01	0.390	4.86
m3 (APL)	2	13.95–15.36	14.66	0.997	6.80
m3 (TW)	2	8.18–8.43	8.31	0.177	1.88

Abbreviations: **APL**, anterior-posterior length; **TW**, transverse width; **TWhyd**, hypoconulid transverse width.

Referred Material—UF 237878, left partial mandible with m1–m3; UF 280223, right m1; UF 267081, left m1.

Diagnosis—Smallest known protoceratine. Differs from all other species of *Paratoceras* in having narrower lower cheek teeth, p3 lacking entostylid, anteriorly wedge-shaped p4 with straight paraconid; and p4 lacking metaconid, posterolabial cuspulid, and anterolingual flexid. Further differs from *P. macadamsi* in having more brachydont cheek teeth, and lacking anterolingual flexid on p3.

Description

Mandible—The holotype includes the posterior part of the horizontal ramus including the alveoli of p2 (Fig. 7A–C). The lingual and labial surfaces of the ramus are mostly uniform (subparallel) below the p4–m3 series but start to narrow (converge) anterior to p3 (Fig. 7B). In lateral view, the ventral margin of the anterior part of the ramus forms an inflected convex margin centered below the p2 alveoli (Fig. 7B). A single anterior mental foramen is preserved in the mandible (UF 271625) beneath the posterior root of p3.

Lower Dentition—The p3 is elongate (APL > TW) and double-rooted. Despite the fact that the protoconid is partially preserved in the only known specimen with a p3, the crown has a well-defined protoconid (Fig. 7A). The conical paraconid is separated from the high and pointed protoconid by a distinct notch, but it lacks an anterolingual flexid. The talonid of p3 is simple, with no evidence of entostylid or any crest associated with the protoconid. The crown of p4 is anteriorly wedge-shaped (with a posterior margin wider than the anterior margin) and remarkably shorter than that of p3 (Table 2). Despite the fact that the crown has little wear, there is no evidence of a distinct metaconid. The crown has a straight and abbreviated paraconid, a high protoconid, and a transversely wide talonid. The talonid is narrow, with a twinned junction of the hypoconid and entoconid forming the posterior-most aspect of the crown and aligned with the protoconid along the midline. There is no labial cuspulid on the posterior margin of the hypoconid of p4 (Fig. 7A).

The lower molars are brachydont, with deep anterior and posterior fossettids (Fig. 7A). The enamel is smooth and lacks strong crenulations. The molars have discontinuous and overlapping crests that appear to intersect after moderate wear. The crescents (hypoconid and protoconid) are asymmetric, with anterior cristids longer than the posterior cristids. Intercolumnar tubercles are barely evident, and restricted to the basal parts of m1 and m2, but are absent on m3 (Fig. 7B). No cingulids are present on the labial margin of the lower molars, and only a well-developed cingulid is visible on anterior margin of the protoconid (Fig. 7B). Despite their brachydont morphology, the molars are relatively narrower (m1 and m2 APL/TW ratio ~1.26) than those of the Barstovian *P. wardi* (m1 and m2 APL/TW ratio ~1.13) and the Hemingfordian *P. coatesi*, sp. nov., from the late Centenario Fauna (m1 and m2 APL/TW ratio ~1.10), but similar to the proportions documented for the Clarendonian *P. macadamsi* (m1 and m2 APL/TW ratio ~1.24). The crowns have well-defined lingual ribs and stylids that are only noticeable in early wear stages, and the metaconid and entoconid are disconnected in all but the most advanced wear stages. The discontinuous and overlapping crests form a distinctive metastylid, and the entostylid consists of a lingual projection of the posterior crescent. Intercolumnar tubercles are faintly developed and restricted to the basal part of the crown between the protoconid and hypoconid (Fig. 7B). Parastylids are well developed on each of the molars, and a distinctive well-developed entostylid is present on the m3 (Fig. 7C). Two enamel ridges compose the hypoconulid of m3. The labial ridge is broader than the lingual, and together they enclose a shallow fossetid (Fig. 7A).

Discussion and Comparisons—The strong paraconid on the elongate p3 and the straight paraconid on p4 of *Paratoceras orarius*, sp. nov., are more similar to those of *Paratoceras* than other early Miocene protoceratids (e.g., synthetoceratines). The shallowest point of the mandible of *Paratoceras orarius* is located below the p3 alveoli, similar to that of taxa classified in Protoceratinae. In synthetoceratines, this mandibular hallmark is located approximately at the midpoint of a distinctive, longer p1–p2 diastema (Patton and Taylor, 1971).

The molar dimensions of *Paratoceras orarius* (Figs. 5, 6) are the smallest among known protoceratines. The ratios of the length of the p3 and p4 relative to the length of the m1 in the holotype indicate that *P. orarius* has an unreduced p3. This hallmark is also present in *Paratoceras* (Frick, 1937:608; Patton and Taylor, 1973) but absent in Synthetoceratinae, which are characterized by more reduced lower premolars with shorter paraconids (Patton and Taylor, 1971). *Paratoceras orarius*, sp. nov., from the early Centenario Fauna is characterized by a narrower lower dentition (Fig. 6; Table 2), with an approximate APLp4/APLm1 ratio of 0.90, whereas *P. wardi, P.* aff. *tedfordi* from the Lirio Norte L. F., *P. coatesi*, sp. nov., and *P. macadamsi* have approximate ratios of 1.02, 1.10, 0.87, and 0.93, respectively.

The lower premolars of *P. orarius* lack the anterolingually directed strong metaconids of *Pseudoprotoceras* (Patton and Taylor, 1973; Emry and Storer, 1981) and the stronger and more inflected paraconids of *P. wardi*. However, the bulbous paraconids of *P. orarius* are more similar to those present in the premolars of the Clarendonian *P. macadamsi* (Patton and Taylor, 1973: fig.13E). Although exhibiting an overall narrower lower dentition (m1 and m2 APL/TW ratio ~1.26), the general morphology of the hypoconulid of the m3 is similar to that of the Barstovian *P. wardi* and the Arikareean *Paratoceras* cf. *P. tedfordi* from the Lirio Norte L. F. The general morphology of the lower dentition of the small-bodied *P. orarius* is similar to that of the larger-bodied Clarendonian *P. macadamsi*; however, this late Miocene higher-crowned protoceratine is characterized by having an elongate p4 with a lingually inflected paraconid and a p3 with strong

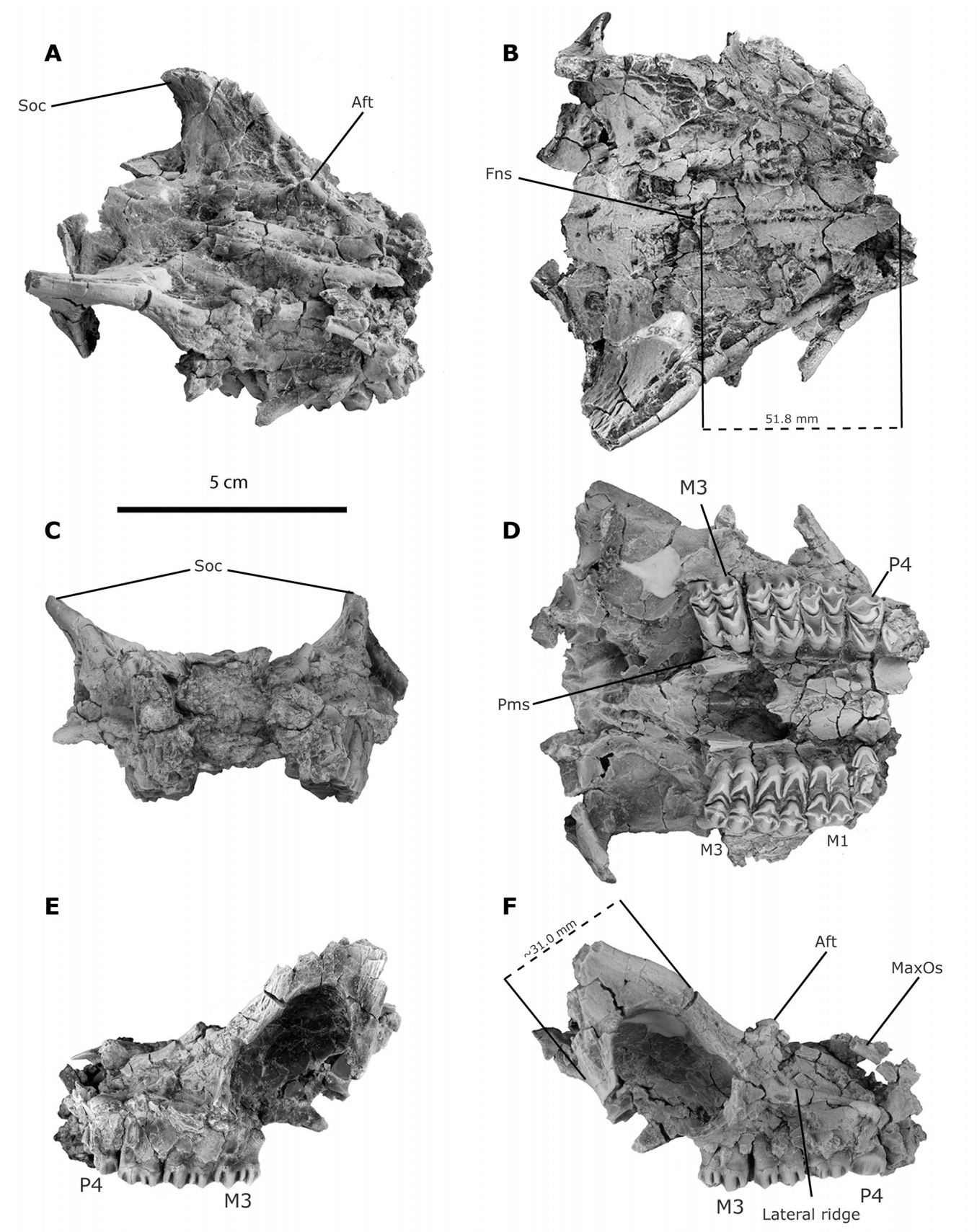

FIGURE 8. Male partial skull of *Paratoceras coatesi* with right P4–M3 and left M1–M3, UF 223585 (holotype). **A**, right oblique view; **B**, dorsal view; **C**, anterior view; **D**, ventral view; **E**, left lateral view; **F**, right lateral view. **Abbreviations**: **Aft**, anterofrontal tuberosity; **Fns**, frontonasal suture; **MaxOs**, maxillary ossicone; **Pms**, maxillary-palatine suture; **Soc**, supraorbital ossicone.

anterolingual flexid and parallel posterior crests that are anteroposteriorly oriented (Patton and Taylor, 1973:fig. 13).

PARATOCERAS COATESI, sp. nov.
(Figs. 8–10; Table 3; Appendix 1)

Protoceratidae: Whitmore and Stewart (1965:182).
Paratoceras, ?new species: Patton and Taylor (1973:368).
Paratoceras wardi: MacFadden (2006:726).
P. wardi Kirby, Jones, and MacFadden (2008:6).

Holotype—UF 223585, incomplete skull that includes partial maxillae with right P4–M3 and left M1–M3, complete nasals, and partial frontal and supraorbital horns.

Locality and Horizon—Escobar Hill (site key YPA-003 in UF Vertebrate Paleontology Collection), Gaillard Cut, Panama Canal area, Panama, Central America (Fig. 1A). The holotype was collected by M. X. Kirby in 2004 (but not previously figured or described) from the same uppermost fossiliferous horizons of the Cucaracha Formation (Fig. 2B) that yielded the Centenario Fauna (MacFadden et al., 2010:fig. 2; Section 8 of Kirby et al., 2008:fig.6). These horizons are correlated to the early Hemingfordian NALMA (He1) (MacFadden et al., 2014).

Etymology—Named in honor of Dr. Anthony G. Coates, Staff Scientist (Emeritus) at the Smithsonian Tropical Research Institute, for his many contributions towards a better understanding of the geology of southern Central America and the timing and consequences of the rise of the Isthmus of Panama.

Paratype—UF 271182, left dentary with p1, p3–m3; right dentary with p1, p3–m3; and symphysis with anterior alveoli. Paratype was recovered from the Centenario 2 locality (site key YPA-060 in UF Vertebrate Paleontology Collection), corresponding to the upper part of the Cucaracha Formation (Fig. 2).

Referred Material—UF 237854, left mandible with Lm1–m3 (Escobar Hill; YPA-003); UF 271624, right mandible with Rp3–m3 (Hodges Hill; YPA-026); UF 223094 (cast of SMU 68102), left mandible with Lp4–m3 (Lirio area; YPA-002); UF 267124, left mandible with Lp4–m3 (Hodges Hill; YPA-026); UF 267123, left mandible with Lp2–m3 and partial symphysis (Hodges Hill; YPA-026); UF 223328 (cast of USNM 23154), right mandible with Rp3–m3; UF 271181, right mandible with Rp1–m2 and partial symphysis (Hodges Hill; YPA-026); UF 267125, left mandible with Lp4 and partial Lm1–m2 (Centenario Bridge; YPA-009); UF 280222, right mandible with Rp3–m2 (Centenario 2; YPA-060); UF 223326 (cast of USNM 23165), partial left maxilla with LM1-M3 (Lirio area; YPA-002); UF 236917, right M3

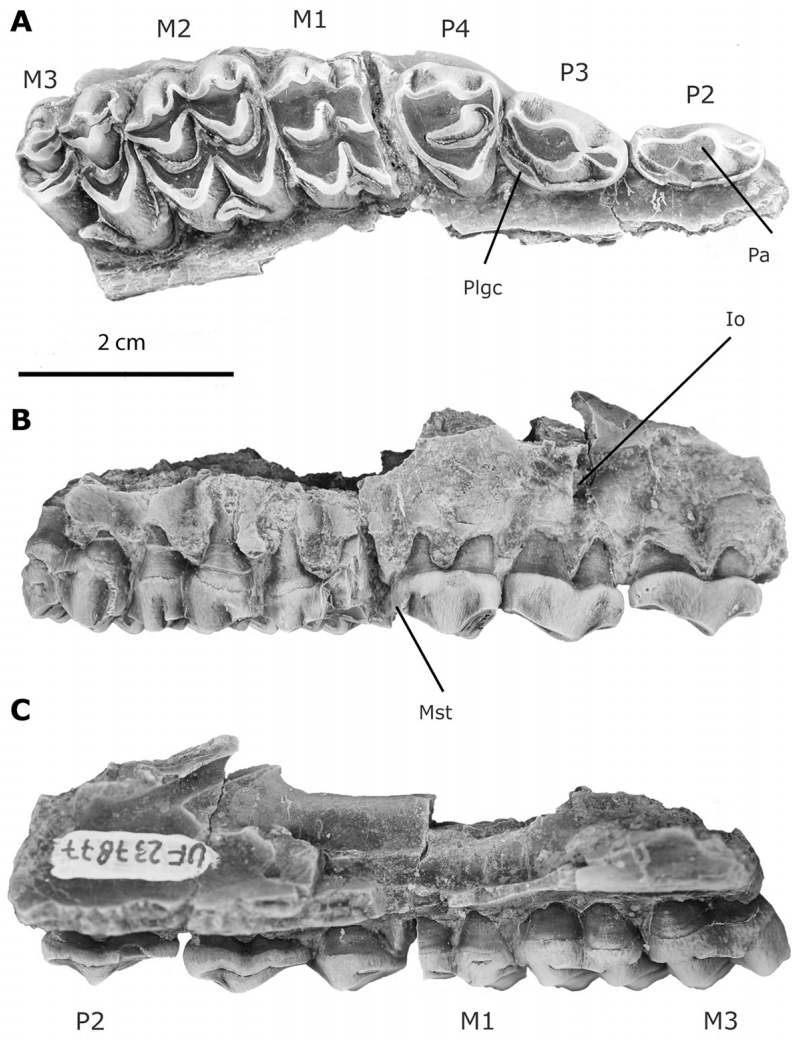

FIGURE 9. Detailed photographs of upper dentition of *Paratoceras coatesi*. UF 237877, right maxilla with P2–M3, **A**, occlusal view; **B**, labial view; **C**, lingual view. **Abbreviations**: **Io**: Infraorbital foramen; **Mst**, metastyle; **Pa**, Paracone; **Plgc**, posterolingual cingulum.

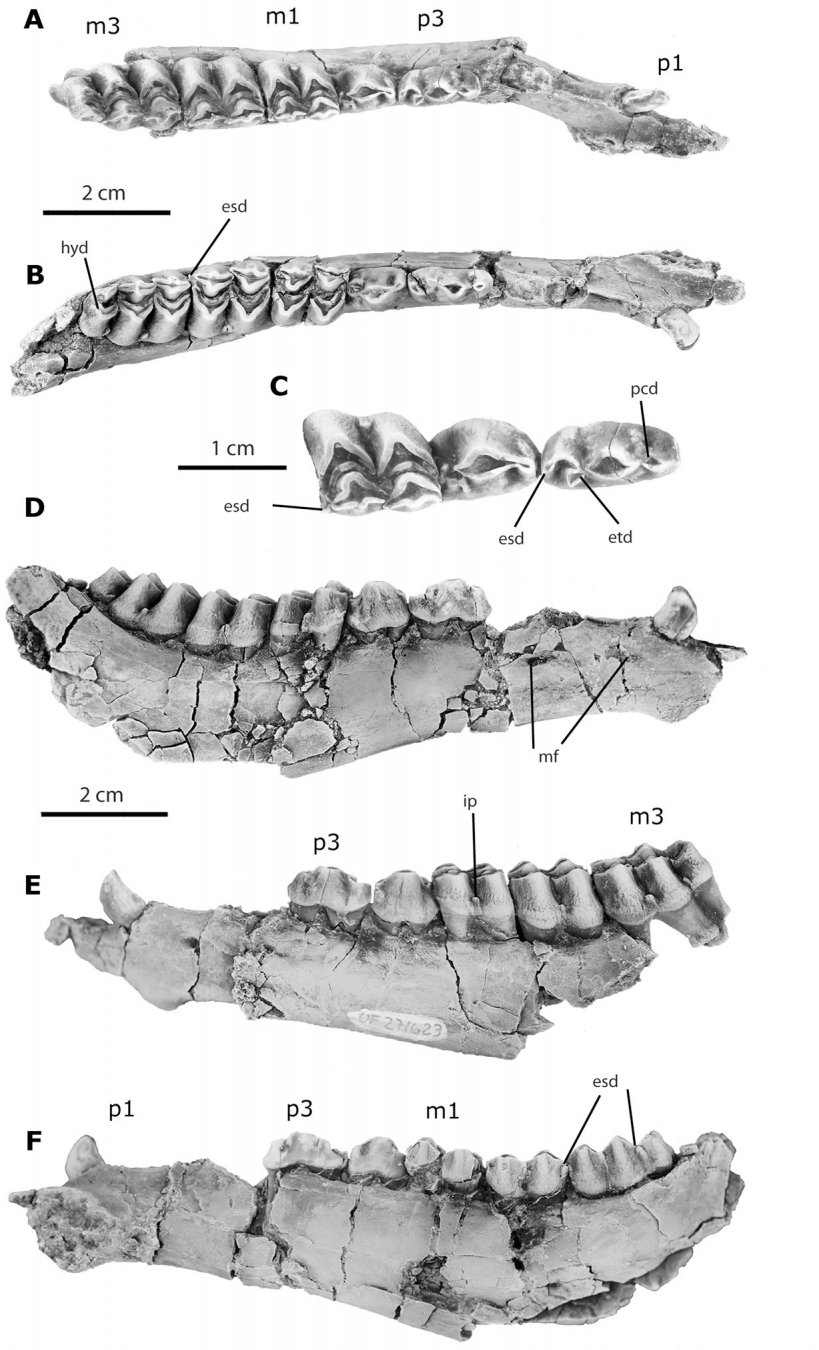

FIGURE 10. Lower dentition of *Paratoceras coatesi*, UF 271182 (paratype), paired mandibles with Rp1, Rp3–m3, Lp1, Lp3–m3, and symphysis. **A**, left dentary with p1, p3–m3, and partial mandibular symphysis, occlusal view; **B**, right dentary with p1, p3–m3, and partial mandibular symphysis, occlusal view; **C**, detail of Lp3–m1, occlusal view; **D**, right mandible with p1, p3–m3, labial view; **E**, left mandible with p1, p3–m3, labial view; **F**, right mandible with p1, p3-m3, lingual view. **Abbreviations**: **esd**, entostylid; **etd**, entoconid; **hyd**, hypoconid; **ip**, intercolumnar pillar; **mf**, mental foramen; **pcd**, paraconid.

(Cartagena Hill; YPA-008); UF 236913, partial right maxilla with RP3 (broken) and Rp4–M1 (Centenario Bridge; YPA-009); UF 223584, partial left maxilla with LP3–M1 (Escobar Hill; YPA-003); UF 280221, right M3 (Centenario Bridge 2; YPA-060); UF 237877, partial right maxilla with RP2–M3 (Centenario Bridge; YPA-009); UF 271180; left partial maxilla with LP4–M3 (Centenario 2; YPA-060); UF 237862, left M1 (Centenario Bridge; YPA-009).

Diagnosis—Differs from all other species of *Paratoceras* in having relatively wider lower premolars with bulbous paraconids; and p3 lacking an anterolingual flexid. Further differs from *P. wardi* in having weaker anterolingual cingular segments on upper premolars, a relatively shorter p4; males have longer nasals, more delicate and low supraorbital ossicones, and more elevated preorbital protuberances. Further differs from *P. teddfordi* in having a relatively narrower P4 and relatively shorter P2–M3 series (~12 % shorter). Further differs from *P. orarius* in having larger teeth, deeper mandible anterior to p3, and relatively wider lower molars. Further differs from *P. macadamsi* in having more brachydont dentition, shallower mandible, and p3 with straighter and weaker paraconid.

Description

Skull—Substantial deformation anterior to the orbits in the partial skull (UF 223585) has artificially reduced the distance

TABLE 3. Summary table of dental measurements (in mm) of *P. coatesi*, sp. nov., from the Cucaracha Formation and *P. wardi* from the Barstovian Trinity River L. F.

Tooth position (Dimension)	N	Range	Mean	Standard deviation	Coefficient of variation
		P. coatesi, sp. nov., lower molars			
p1 (APL)	2	6.26–6.36	6.31	0.071	1.12
p1 (TW)	2	3.55–3.62	3.59	0.049	1.36
p2 (APL)	1	13.74	—	—	—
p2 (TW)	1	6.10	—	—	—
p3 (APL)	5	12.30–13.99	13.12	0.714	5.44
p3 (TW)	5	5.25–6.45	6.09	0.482	7.91
p4 (APL)	7	8.95–10.76	10.21	0.656	6.42
p4 (TW)	7	6.5–7.93	7.46	0.470	6.30
m1 (APL)	9	10.26–12.29	11.71	0.598	5.11
m1 (TW)	9	8.81–11.69	10.41	0.914	8.78
m2 (APL)	6	12.36–14.54	13.36	0.723	5.41
m2 (TW)	6	11.73–13.39	12.38	0.646	5.20
m3 (APL)	7	17.38–20.62	18.31	1.050	5.73
m3 (TW)	7	9.90–12.72	11.45	0.894	7.81
m3 (TWhyd)	7	6.53–7.15	6.92	0.205	2.96
		P. coatesi, sp. nov., upper molars			
P2 (APL)	1	12.63	12.63	—	—
P2 (TW)	1	6.18	6.18	—	—
P3 (APL)	2	11.79–12.65	12.22	0.61	4.97
P3 (TW)	2	8.46–8.58	8.52	0.084	0.98
P4 (APL)	4	7.79–9.41	8.56	0.710	8.27
P4 (TW)	4	11.53–13.83	12.78	1.060	8.29
M1 (APL)	6	10.81–11.37	11.09	0.202	1.82
M1 (TW)	6	14.48–15.03	14.71	0.820	5.57
M2 (APL)	5	11.29–12.83	12.36	0.720	5.83
M2 (TW)	5	14.34–17.94	16.73	1.463	8.72
M3 (APL)	7	11.63–13.58	12.51	0.803	6.41
M3 (TW)	7	16.18–17.65	16.7	0.653	3.91
		P. wardi lower molars			
p2 (APL)	2	12.13–12.42	12.28	0.205	1.67
p2 (TW)	2	4.30–4.48	4.39	0.127	2.89
p3 (APL)	3	11.96–13.22	12.57	0.631	5.02
p3 (TW)	3	4.94–5.15	5.02	0.116	2.31
p4 (APL)	7	10.05–12.01	11.27	0.583	5.17
p4 (TW)	7	6.19–7.01	6.68	0.311	4.66
m1 (APL)	9	10.57–11.53	11.00	0.354	3.22
m1 (TW)	9	8.08–10.32	9.34	0.476	5.09
m2 (APL)	9	10.88–12.5	11.95	0.524	4.38
m2 (TW)	9	10.16–11.00	10.58	0.344	3.25
m3 (APL)	8	10.43–18.56	17.67	0.789	4.46
m3 (TW)	8	10.67–11.22	10.89	0.196	1.80
m3 (TWhyd)	8	5.99–7.02	6.42	0.318	4.95
		P. wardi upper molars			
P2 (APL)	2	13.01–13.02	13.02	0.007	0.05
P2 (TW)	2	6.53–6.61	6.57	0.057	0.86
P3 (APL)	4	11.42–13.15	12.65	0.82	6.48
P3 (TW)	4	7.31–8.60	8.01	0.61	7.61
P4 (APL)	5	9.03–9.83	9.41	0.309	3.28
P4 (TW)	5	11.64–12.45	12.00	0.301	2.51
M1 (APL)	6	11.01–11.89	11.45	0.352	3.07
M1 (TW)	6	12.86–13.95	13.41	0.438	3.26
M2 (APL)	5	11.93–12.98	12.44	0.408	3.28
M2 (TW)	5	15.05–16.12	15.68	0.453	2.89
M3 (APL)	4	12.78–13.15	12.85	0.233	1.83
M3 (TW)	4	14.81–16.82	16.03	0.942	5.87

Abbreviations: **APL**, anterior-posterior length; **TW**, transverse width; **TWhyd**, hypoconulid transverse width.

between the frontals and maxillae in lateral views (Fig. 8). The frontals, which have an anterior contact with the nasals, are large and wide massive bones (Fig. 8A, B). The partially preserved supraorbital ossicones are composed exclusively from a prolongation of the frontal bones. The anteroposterior length of the base of the ossicone at the level of the roof of the orbit is 31.0 mm, and it rises to a height of approximately 50.0 mm above the base (length/height ratio: ~0.62). The proximal (basal) segment of each ossicone is flared (Fig. 8A–C), whereas the partially preserved distal aspect is characterized by a tapering and blunted triangular morphology. The supraorbital ossicones, although partially deformed, are gently medially recurved and narrow gradually from the base up to the posteriorly recurved distal end. The dorsal surface of the frontal is rugose, with deep grooves, pits, and numerous small foramina (Fig. 8B). Similar rugosity is also present on the dorsal surface of the nasal and maxillary bones. The suture of the frontals forms a low but distinctive sagittal ridge that ends at the nasofrontal suture. From this point, a small ridge extends laterally to form a longitudinal deep pit anterior to a large and distinct fossa located in the posterior part of the nasal bone. This pit extends from the posteromedial end of the nasal to the anteromedial end of the second conical pair of maxillary protuberances located above the M2 (Fig. 8A, B). These tuberosities at the lateral junction (left and

right) of the frontal and nasal resemble a distinctive pair of small ossicones (Fig. 8A, E, F). The sutures surrounding the nasals are clearly distinct. The nasals contact the dorsal margin of the maxillae for most of their length (~52 mm on the median line), ending anteriorly at the level of P3, with short, anterior, wedge-like projections that join at the midline (Fig. 8B). The nasals widen posteriorly, with their widest point at the contacts with the lacrimals. The dorsal surface of the nasals has two deep longitudinal grooves that lead posteriorly to supraorbital foramina in the frontals. Although the suture with the zygomatic is not preserved, a descending process from the frontal partially closes the orbit posteriorly (Fig. 8E, F). In lateral view, the anterior part of the lacrimal contacts the maxilla ventrally and the nasal and frontal dorsally, and the posterior lacrimal contacts the frontal forming a conical protuberance (Fig. 8E, F). Three lacrimal foramina are located within the orbital anterior border. The palatine bones are flat and narrow (Fig. 8D) and are anteriorly bounded by the maxillary bones. In ventral view, the suture between the palatine bones and the maxillary bones is at the level of the roots of M1 (Fig. 8D). The maxillary-palatine suture projects from the midline labially and curves posteriorly as it approaches the posterior root of M2. In ventral view, a reduced palatine bone surrounds the internal nares. The palatine bones are restricted to a thin rim of the choanal border, and their suture with the maxillary bones extends forward from the lingual part of the M3 alveoli, reaching the maxillary suture lingual to M2. The anterior end of the internal nares in the palate is located at the level of the posterior root of M2. The orbits are large, suboval in outline, and widely separated from each other. The anterior margin of the orbit is above the M3. The roof of the orbit gives rise to the supraorbital ossicones (Fig. 8E, F).

The partially preserved anterior ossicones are formed entirely by an expansion of the maxillary bones. They project above P4 and seem to be located behind the anterior end of the nasals (Fig. 8A, E, F). A strong lateral ridge is partially preserved in the right maxilla (Fig. 8F). This ridge roughly starts above P4, forming a prominent tubercle and continuing posteriorly to the anterior margin of the orbit. The posterior narial notch is posterior to the maxillary-palatine suture and is located between the palatine and the pterygoid. The maxillary plates form the roof of the palate.

Upper Dentition—The crowns of P2, P3, and P4 are better preserved in UF 237877 (Fig. 9) than in the holotype (UF 223585) and form the basis for much of the description here. The P2 is tri-rooted, with the lingual root located close to the posterolabial root. The crown is elongate (APL > TW), lacks external ribs, and has a distinct paracone interrupting an internal cingulum (Fig. 9A). This cingulum widens posteriorly and encloses a small open basin lingual to the metastyle. The labial margin of the crown is straight, with the parastyle, paracone, and metastyle anteroposteriorly aligned. The anterolingual crescent is low and formed by a distinct small cingular segment. The posterolingual crescent is also low and formed by a small cingular segment that extends lingually from the base of the paracone towards the posterior margin of the crown.

The crown of P3 resembles that of P2 in general morphology. The P3 (Fig. 9A) is also tri-rooted, but with a more lingually expanded crown posterior to its midpoint (forming a more distinct 'wedge shape') than that of P2. The crown of P3 further differs from that of P2 in having a distinctively higher and stronger paracone, a less distinct metastyle that is slightly recurved labially, and an internal cingulum that is more nearly continuous and reaches the labial segments of both the parastyle and the mesostyle. The internal cingulum forms a narrow valley anterior to the lingual surface of the paracone (Fig. 9A–C) and a wider valley on the posterior margin of the paracone. Whereas the labial contour of the crown is straight (the parastyle, paracone, and metastyle are aligned), the lingual cingular segment is simple, with no evidence of a functional protocone.

The crown of P4 (Fig. 9A) is triangular (labial longer than lingual margin) and submolariform, with the development of a crescent but lacking a metacone and hypocone. The metastyle is more prominent and more labially recurved than the parastyle. The crescent is asymmetric, with a shorter anterior crista that is responsible for a forwardly placed protocone. The internal cingulum varies from a continuous, well-developed basal cingulum to basal cingular segments that are not continuous and are restricted to the anterior and posterior labial portions of the crescents. The upper molars are wider than they are long and have crenulated enamel (Table 3; Fig. 6). The M1 and M2 have strong stylar cusps on the anterior and posterior crests. The internal cingulum of the upper molars is similar in its variable continuity to that of P4. For example, the holotype (UF 223585) has a strong continuous cingulum along the anterior and posterior margins of each upper molar. It projects from just above the base of the crown and extends along the anterior or posterior basal part of each crescent. On the other hand, these internal cingula are not continuous in UF 237877, but interrupted by the protocone and metaconule. The crowns of M1 and M2 are rectangular (transversely elongated) in occlusal outline, whereas M3 has a more squared outline with a transversely reduced posterior margin (Fig. 9A). Both M1 and M2 have prominent mesostyles and strong ribs extending up each crest from the base of the crown to the tip of both the paracone and metacone (Fig. 9C). The shape of the crescents varies from an open 'V' or 'U' (towards the labial margin) in the posterior molars to a more closed 'V' on M1. The crescents of M1 and M2 are asymmetric, with relatively shorter anterior cristae that are responsible for a more forwardly placed protocone and metaconule (Fig. 9A). In UF 237877, the crests of M3 (paracone and metacone) are aligned and more or less continuous, resulting in the absence of a mesostyle, whereas in the holotype (UF 223585), the mesostyle is well developed (Figs. 8D, 9A). However, in both specimens, the anterior crescent of the crown of M3 is remarkably wider than the posterior one, which is extremely reduced transversely.

Mandible—Well-preserved and associated left and right dentaries are described here and included as a paratype (UF 271182) of *Paratoceras coatesi*. The horizontal ramus is slender and gradually shallows anterior to m1 in lateral view (Fig. 10). Whereas the lingual and labial surfaces of the ramus are uniform below the p4–m3 series, the mandible is ventrally recurved anterior to p3 and flares labially anterior to p2 in occlusal view (Fig. 10A, B). The p1 is separated from the incisors by an anterior diastema that appears to be short, but the exact length is unknown because of poor preservation in that region. The crown of p1 is further separated posteriorly from that of p2 by what appears to be a longer diastema subequal to the length of the p3 (Fig. 10D). The dorsal edges of the p1–p2 diastema are sharp and pinched below the edge forming a well-defined crest. The mandibular symphysis is unfused, oval, short, and deep, with a distinct ventral projection beneath p1 (Fig. 10D–F). Two small mental foramina are present, one beneath the posterior alveolus of p3 and the other beneath the p1–p2 diastema (Fig. 10D).

Lower Dentition—In none of the specimens are the incisors or their alveoli anterior to p1 preserved. The first premolar is caniniform, single-rooted, and posteriorly recurved (Fig. 10A, B). Both the lingual and labial surfaces are convex and lack crenulations or additional cusps. The crown is distally elongate, with a small ridge on the basal posterior part of the crown that extends to the apical posterior tip and an anterior ridge that extends up the anterior edge of the crown interrupted by a moderately developed wear facet for about half its length (Fig. 10B). Dentine is exposed on the occlusal wear surface as a narrow band on the anterior margin of the enamel. Although severely affected by deformation and wear, the only p2 available for description is that reported in UF 271181 (see referred specimens). The p2 is double-rooted and subequal to the length of the p3

(Appendix 1). The crown is elongate (APL > TW), with a distinct paraconid separated from the protoconid by a notch. In all general morphologies preserved, the p2 is comparable to the p3 of the paratype (Fig. 10C), differing only from the latter in having a narrower talonid.

The p3 is elongate and has a distinctive bulbous and more robust crown than that of the p2 (Fig. 10C). It is double-rooted, with an abbreviated paraconid, an acute apex (metaconid), and a more developed talonid than that of p2. The paraconid is separated from a high and conical protoconid by a distinct notch, with no evidence of an anterolingual flexid. The talonid makes up about one-third of the crown of p3 and forms a distinctive open valley with distinct entoconid and entostylid on its lingual margin. In occlusal view, the crown of p4 is anteriorly wedge-shaped. The posterior segment (talonid) is wider than the anterior segment and fashioned by a labial cuspulid. The paraconid of p4 is narrow, lingually inflected, and forms a lingual anteroflexid. The metaconid, only evident in early wear stages, is situated high on the crown and close to the protoconid, resulting in a relatively short, high-crowned, and bulbous tooth (Fig. 10C). The entoconid and entostylid are located on small crests that project parallel to each other, forming a posterolingually open valley. This valley is present in early wear stages, but with progressive wear the talonid becomes a narrow crest directed posteriorly. The lower molars are brachydont, weakly crenulated, and have well-developed anterior and posterior fossettids. The crests of the metaconid and entoconid are not connected, and the posterior end of the metaconid overlaps the anterior end of the entoconid (Fig. 10A–C). The parastylid is formed by the lingual expression of the anterolingual cristid of the paraconid, but this morphology is only evident in the early stages of wear. Parastylids are slightly developed in m1 and m2 and barely discernible on the anterior crest of m3. Intercolumnar pillars are restricted to the basal part of the labial aspect of the crown between the protoconid and hypoconid on m1 and m2 and are variably present on m3 (Fig. 10D, E). A distinctive entostylid is present in the lingual surface of m3 (Fig. 10C). Two ridges divide the hypoconulid of m3, forming a double enamel loop on the talonid of m3 that encloses a fossetid (Fig. 10A, B).

Discussion and Comparisons—Although the diagnostic occipital forked ossicone found in male specimens of *Paratoceras* is not preserved in the holotype of *P. coatesi*, many informative characters are otherwise evident. The skull of *Paratoceras coatesi* has a number of diagnostic protoceratine characteristics that are also present in the male skull of *P. wardi* from the Barstovian Trinity River L. F. in Texas but absent in *Protoceras*. These include (1) flared supraorbital horns that are triangular in cross-section with a rugose anterior edge; (2) more forwardly placed orbits than those of *Protoceras* and *Pseudoprotoceras*; (3) maxillary protuberances that arise more posteriorly than those of *Protoceras*; and (4) nasals retracted to the level of P3. The dentition resembles that of *P. wardi* in having (1) upper molars that are wider than long; (2) variable expression of the internal cingula (from strong and continuous to weak and discontinuous) on the upper molars; (3) lack of a distinctive protocone on P2 and P3; and (4) the labial surface of P2 and P3 straight, with no evidence of the labially projected parastyle that is present in *Protoceras* and *Pseudoprotoceras*.

In contrast to *Paratoceras wardi*, the more gracile morphology of the supraorbital ossicones of *Paratoceras coatesi* and the second and stronger conical pair of maxillary protuberances above the lacrimals are the most distinctive hallmarks preserved in the partial male skull. *P. coatesi* differs from *P. wardi* in having weaker anterolingual cingular segments on upper premolars, more bulbous (relatively wider and shorter) lower premolars (Fig. 5; Table 3), a p3 lacking an anterolingual flexid between the paraconid and the protoconid, more delicate supraorbital horns (length/height ratio for *P. coatesi* is ~0.62 vs. ~0.70 for *P. wardi*), longer nasals (nasal median length/APLM1–M3 ratio for *P. coatesi* is ~1.32 vs. ~0.94 for *P. wardi*), and more pronounced conical protuberances at the lateral junctions of the frontal and nasal in males (Patton and Taylor, 1973:fig.5, table 4). *P. coatesi* (male) has longer nasal bones than those of the holotype of *P. tedfordi* (female), as was previously noticed for *Protoceras* (Marsh, 1897). Although only known from a female upper dentition, the P4 of *Paratoceras tedfordi* is wider than the M1 (Webb et al., 2003:table 14.1) whereas in *P. coatesi*, the P4 is narrower than the M1 (Fig. 6). Although the general morphology of the crown of the p4 and the lower molars of *P. coatesi* are similar to that of *P. macadamsi*, it lacks the higher crowns and deeper mandible characteristic of the larger Clarendonian protoceratine. *Paratoceras coatesi*, sp. nov., from the Centenario Fauna has an approximate APLp4/APLm1 ratio of 0.87, whereas *P. wardi, P. orarius*, sp. nov., *P.* aff. *tedfordi* (Lirio Norte L. F.), and *P. macadamsi* have ratios of 1.02, 0.90, 1.10, and 0.93, respectively.

The general morphology of the cingula on the upper dentition and the development of a mesostyle on the upper M3 of *Paratoceras coatesi* are variable. The cingula vary from more nearly continuous around the P4–M3 series in the holotype (Fig. 9) to discontinuous cingular segments, more restricted to the lingual opening of the transverse valley in the referred specimens and are interrupted by the protocone and the metaconule. However, the posterolingual cingular segments are predominantly more developed than the anterior counterparts in the upper premolars (P2–P3). The morphology of the M3 metastyle is also variable in specimens with comparable tooth dimensions in the *P. coatesi* specimens. Besides its distinctively wider and bulbous lower premolars and a P4 that is narrower than the M1, *P. coatesi* is most similar to *P. tedfordi* in all other comparable morphologies preserved in the holotype of *P. tedfordi*.

PHYLOGENETIC ANALYSIS

To evaluate the phylogenetic relationships of the new fossil species from Panama, we performed a cladistic analysis of 10 protoceratine taxa, with the primitive protoceratid *Heteromeryx dispar* from the Chadronian of Texas and the Great Plains as the outgroup (Fig. 11; Appendix 3). Because most protoceratid species are not known from large samples of fossils that preserve cranial morphology, mainly dental (12) and only a few cranial (3) characteristics that presumably do not exhibit a marked sexual dimorphism (Appendix 2) were scored and used in our analysis. Morphological data were compiled from a study of specimens and a literature review (Appendix 2). The data matrix (Appendix 3, Supplementary Data) includes characters that are unordered and weighted equally, and characters not known for a taxon were coded as missing. Data were compiled in Mesquite version 2.72 (Maddison and Maddison, 2009) and then analyzed under the parsimony criterion using the branch and bound algorithm of PAUP version 4.0b10 (Swofford, 2003). The analysis resulted in a single equally most parsimonius cladogram (MPT) with a tree length of 24 steps, a consistency index (CI) of 0.875, a retention index (RI) of 0.889, and a homoplasy index (HI) of 0.125 (Fig. 11).

Our results support a monophyletic *Paratoceras* (node 4), based on the presence of strongly retracted nasals (1[1]); P3 protocone reduced to a basal cingular segment interrupted by an inflated paracone (3[2]); orbits located anterior to the posterior roots of the M3 (6[1]); and a P3 with a straight labial margin lacking enlarged labial styles (12[1]). The Arikareean *P. tedfordi* from southern Mexico appears as the most primitive species of the genus.

In our resulting topology, *Paratoceras* aff. *P. tedfordi* from the Lirio Norte L. F. appears as the sister taxon of the Hemingfordian, Barstovian, and Clarendonian *Paratoceras* spp. These relationships are based exclusively on the presence of relatively

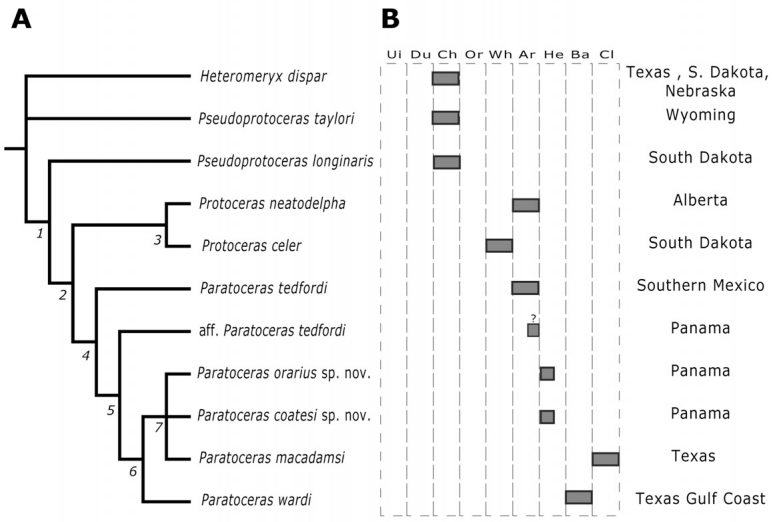

FIGURE 11. Hypothetical relationships of the early Miocene protoceratines from Panama within Protoceratinae based on a 15-character matrix with *Heteromeryx dispar* as the outgroup. **A**, strict consensus tree resulting after analysis under the parsimony criterion using the branch and bound algorithm of PAUP* version 4.0b10 (Swofford, 2003) (tree length = 24; CI = 0.875, RI = 0.885, HI = 0.125); **B**, biostratigraphic distribution of the protoceratids included in the phylogenetic analysis. **Abbreviations**: **Ar**, Arikareean Faunal Zone; **Ba**, Barstovian Faunal Zone; **Ch**, Chadronian Faunal Zone; **Cl**, Clarendonian Faunal Zone; **Du**, Duchesnean Faunal Zone; **He**, Hemingfordian Faunal Zone; **Or**, Orellan Faunal Zone; **Ui**, Uintan Faunal Zone; **Wh**, Whitneyan Faunal Zone. At each node (bold numbers), the supporting unambiguous synapomorphies are **1**, Protoceratinae (?) (4 [2]); **2**, (5[1] DELTRAN, 7[1], 13[1], 15[1]); **3**, *Protoceras* (4[1], 9[1]); **4**, *Paratoceras* (1[1], 3[2], 12[1], 6[1]); **5**, (2[1]); **6**, (7[2], 8[1], 10[1], 14[1]); **7**, (9[1], 13[2]).

wider upper molars of this taxon (node 5, 2[1]). Although new fossil discoveries are needed from low latitudes, the current distribution suggests that *P. tedfordi* could represent the ancestral stock that gave rise to the protoceratine radiation in tropical Central America. The remaining species of *Paratoceras* with tropical and subtropical distributions include the Hemingfordian *P. orarius* and *P. coatesi* from Panama, and the Clarendonian *P. macadamsi* and the Barstovian *P. wardi* from Texas (node 6) sharing a reduced p4 protoconid that forms a narrow valley with the hypoconulid (7[2]); relatively wider p4 (8[1]); m1 that is longer than p4, APLm1/APLp4 ratio >1 (10[1]); and hypoconid reaching the metaconid on p3 (14[1]).

Within *Paratoceras*, the Hemingfordian forms from Panama, *P. orarius* and *P. coatesi*, are grouped with the Clarendonian *P. macadamsi* (node 7), based on the lack of a strong parastylid on the lower molars (9[1]) and the more reduced p4 talonid with a shallow fossetid (13[2]). The Barstovian *P. wardi* and the late Arikareean *P.* aff. *tedfordi* from the Lirio Norte L. F. are excluded in part based on having a longer p4, a morphological feature shared with *Protoceras* and the remaining members of the genus (node 2, (13[1])). The late Oligocene–early Miocene *Protoceras* appears as the sister taxon of *Paratoceras tedfordi* (node 2) based on the presence of a lateral ridge extending from the outer face of the maxillary bone to the orbit (5[1] DELTRAN); reduced p4 talonid with divergent entoconid and divergent entostylid (13[1]); reduced p4 protoconid forming an open valley with the hypoconid (7[1]); and presence of a paraconid on p3 (15[1]). The late Oligocene *Protoceras celer* forms a clade with similarly aged (Arikareean) *Protoceras neatodelpha* (node 3) based on the presence of anterolingual cingula on the upper molars (4[1]) and the presence of weak parastylids on the lower molars (9[1]).

DISCUSSION AND CONCLUSIONS

The early Miocene fossil record of Panama includes three species of protoceratines, all classified in the genus *Paratoceras*. Protoceratine fossils from the late Arikareean Lirio Norte L. F. are referred to *Paratoceras* aff. *P. tedfordi* based on the morphological characteristics of the upper dentition shared with that early Miocene species from Mexico. The small protoceratid *Paratoceras orarius* (initially reported as *P. wardi*, Kirby et al., 2008:fig. 6) is restricted to the lowermost stratigraphic levels of the Centenario Fauna and was found in sedimentary sequences believed to represent deltaic (delta front) and transitional environments (Upper Culebra Formation). The medium-sized *P. coatesi* (previously referred to *P. wardi* by MacFadden, 2006) is the most common ungulate recovered from the late Centenario Fauna. These stratigraphic levels of the upper Cucaracha Formation may have represented more proximal deltaic plains (Kirby et al., 2008; Montes et al., 2012).

Results of a cladistic analysis of 11 protoceratine species, using 15 craniodental characters, suggest that *Paratoceras* is closely related to the Oligocene to early Miocene genus *Protoceras*, with early Miocene *Paratoceras tedfordi* from the Arikareean NALMA of Mexico and likely Panama (*P.* aff. *tedfordi*) as the basal members of the genus. The geographic distribution of species classified in the monophyletic *Paratoceras* clade is consistent with the idea that the group as a whole was endemic to subtropical and tropical areas of the Gulf Coast, Mexico, and Panama and became an abundant component of ungulate faunas from southern Central America by the Hemingfordian after colonizing recently emerged volcanic terrains connected to the Gulf Coast during the Arikareean. *Paratoceras* persisted in the tropical forests of Panama (Graham, 1999a) during the early Miocene (Hemingfordian NALMA), reaching the more temperate forest of Texas by the Barstovian NALMA (Patton and Taylor, 1973). By the late Miocene (Clarendonian NALMA), *Paratoceras macadamsi* had evolved a more wedge-shaped p4, more reduced premolars, deeper mandible, and a more hypsodont dentition; these are all characteristics that are also found in synthetoceratine protoceratids (which are unknown south of Mexico; Webb et al., 2003). Although it is certainly possible that these dental innovations (and inferred dietary specializations) are related to paleoecological changes in the Gulf Coast during the late Miocene, testing this hypothesis would require detailed dietary, isotopic, and phytogeographic studies that are beyond the scope of this project.

The broad snout and brachydont dentitions of protoceratines (e.g., *Paratoceras*) are consistent with those of folivorous browsers with less cursorial morphological traits such as short limbs, unfused metapodials, and four-toed manus. As such, protoceratines might have been restricted to more closed forest, and

presumably more tropical, habitats of southern Mexico and Panama (Prothero, 1998; MacFadden and Higgins, 2004; Jaramillo et al., 2014), whereas the more hypsodont synthetoceratines likely inhabited more open habitats in the Gulf Coast during the Neogene (Webb et al., 2003).

The only species of *Paratoceras* known from male skulls are *P. coatesi* and *P. wardi*. Although far from resolved given the paucity of data, morphological characters present in the male skull of *P. coatesi* (longer nasal bones and the more gracile morphology of the supraorbital ossicones than those of *P. wardi*) are intermediate between those of late Oligocene–early Miocene *Protoceras celer* and Barstovian *Paratoceras wardi* from Texas. In a temporal preliminary framework, this morphological interpretation is consistent with a Hemingfordian age (He1) for the Centenario Fauna (Tedford et al., 2004; MacFadden, 2006; MacFadden et al., 2014).

Webb et al. (2003) suggested that *P. tedfordi* from Mexico is late Oligocene–early Miocene in age, but a younger proposed age (Solórzano-Kraemer, 2007, 2010; Vega et al., 2009) could account for the similarities to *P.* aff. *P. tedfordi* from the late Arikareean Lirio Norte L. F. documented here. The new protoceratines from the Hemingfordian Centenario Fauna (*Paratoceras orarius* and *P. coatesi*) share a distinctive p4 morphology (relatively wider and shorter crown) not present in either Barstovian *P. wardi* or Arikareean *P. aff. P. tedfordi* but present in the Clarendonian *P. macadamsi*. Although this conclusion is tentative, especially with the lower dentition of *P. tedfordi* still unknown, we suggest the possibility that allopatric speciation of *Paratoceras* in different paleobiogeographic provinces (e.g., tropical vs. subtropical) may have occurred in Central America.

Although an early Miocene migration of herpetofauna between the Americas has been proposed prior to the complete emergence of the Isthmus of Panama (Cadena et al., 2012; Head et al., 2012; Hastings et al., 2013), to date no early Miocene terrestrial mammals from Panama have been published that provide evidence of South American taxa in the Panamanian basin despite its proximity to South America (MacFadden, 2006). Furthermore, the faunal content of both the Lirio Norte L. F. and the Centenario Fauna is dominated by mammalian clades endemic to North America (Whitmore and Stewart, 1965; MacFadden, 2006; Rincon et al., 2012b). Among these early Miocene Panamanian clades, the protoceratines, the floridatraguline camels, and the anthracotheres show taxonomic affinities to subtropical taxa from the Gulf Coast and southern Mexico (Rincon et al., 2012a, 2013). On the other hand, ungulates such as equids, oreodonts, moschids, rhinoceroses, and the amphicyonine carnivores expanded their latitudinal distribution from the late Oligocene, spreading in the early Miocene from the Holarctic temperate sequences to the tropical areas of Panama (MacFadden, 2009; Rincon et al., 2012b; MacFadden et al., 2014). Ongoing paleontological work, as well as new geological interpretations (Farris et al., 2011; Montes et al., 2012; Coates and Stallard, 2013) about the tectonic evolution of southern Central America, offer a new paleogeographic model to further explore the diversification processes that might have affected terrestrial vertebrates that colonized the volcanic terrains that emerged during the late Oligocene and early Miocene in the southern part of North America.

ACKNOWLEDGMENTS

We thank J. Bourque and D. Byerley at the FLMNH who prepared fossil specimens in the laboratory, and C. Montes, S. Suarez, M. Vallejo, and F. Moreno (STRI) and G. S. Morgan, A. Wood, J. Carr, S. Lukowski, D. Jones, J. Velez-Juarbe, and B. Newstead (PCP-PIRE) who helped collect the specimens. Special thanks to R. Hulbert Jr. (FLMNH) for help with anatomical terminology and taxonomic nomenclature. Thanks also to the AMNH staff for access to relevant fossil specimens, and K. Cummings, J. Pardo, and C. Byrd who edited an earlier version of the manuscript and made helpful comments for its improvement. Thanks to R. Emry and one anonymous reviewer for helpful reviews and comments that improved the quality of the manuscript. We also thank the Panama Canal Authority (ACP) and the Ministerio de Comercio e Industria (MICI) for access to relevant fossil sites and the UF Department of Geological Sciences for its support. This research was supported by UF Research Opportunity Grant; the U.S. National Science Foundation Partnerships in International Research and Education grant 0966884 (OISE, EAR, DRL), EAR 0824299, and EAR 0418042; National Science Foundation's Advancing Digitization of Biodiversity Collections Program (iDigBio) NSF EF 1115210; STRI-Tupper Paleontological Fund; STRI-Panama Canal Authority Fund; and Ricardo Perez Toyota, Panama. This is UF Contribution to Paleobiology number 660.

LITERATURE CITED

Albright, L. B., III. 1998. The Arikareean Land Mammal Age in Texas and Florida: southern extension of the Great Plains and Gulf Coastal Plain endemism; pp. 167–183 in D. O., Terry Jr., H. E. LaGarry, and R. M., Hunt Jr. (eds.), Depositional Environments, Lithostratigraphy, and Biostratigraphy of the White River and Arikaree Groups (Late Eocene to Early Miocene, North America). Geological Society of America Special Paper 325, Boulder, Colorado.

Albright, L. B., III. 1999. Ungulates of the Toledo Bend Local Fauna (late Arikareean, early Miocene), Texas Coastal Plain. Bulletin of the Florida Museum of Natural History 42:1–80.

Albright, L. B., III, M. O. Woodburne, T. Fremd, C. C. Swisher III, B. J. MacFadden, and G. R. Scott. 2008. Revised chronostratigraphy and biostratigraphy of the John Day Formation (Turtle Cove and Kimberly members), Oregon, with implications for updated calibration of the Arikareean North American Land Mammal Age. Journal of Geology 116:211–327.

Barbour, E. H. 1905. A new Miocene artiodactyl. Science 22:797–798.

Black, C. C. 1978. Paleontology and geology of the Badwater Creek area, central Wyoming. Part 14: the artiodactyls. Annals of the Carnegie Museum 47:223–259.

Cadena, E., J. Bourque, A. Rincon, J. I. Bloch, C. Jaramillo, and B. MacFadden. 2012. New turtles (Chelonia) from the Late Eocene through Late Miocene of the Panama Canal Basin. Journal of Paleontology 86:539–557.

Coates, A. G., and R. F. Stallard. 2013. How old is the Isthmus of Panama? Bulletin of Marine Oceanography 89(4):801–813. doi: 10.5343/bms.2012.1076.

Cook, H. J. 1934. New artiodactyls from the Oligocene and lower Miocene of Nebraska. American Midland Naturalist 15:148–165.

Emry, R. J., and J. E. Storer. 1981. The hornless protoceratid *Pseudoprotoceras* (Tylopoda: Artiodactyla) in the early Oligocene of Saskatchewan and Wyoming. Journal of Vertebrate Paleontology 1:101–110.

Farris, D. W., C. Jaramillo, G. Bayona, S. A. Restrepo-Moreno, C. Montes, A. Cardona, A. Mora, R. J. Speakman, M. D. Glascock, and V. Valencia. 2011. Fracturing of the Panamanian Isthmus during initial collision with South America. Geology 39:1007–1010.

Frick, C. 1937. Horned ruminants of North America. Bulletin of the American Museum of Natural History 69:1–669.

Gazin, C. L. 1955. A review of the upper Eocene Artiodactyla of North America. Smithsonian Miscellaneous Collections 128:1–96.

Graham, A. 1985. Studies in Neotropical paleobotany. IV. The Eocene communities of Panama. Annals of the Missouri Botanical Garden 72:504–534.

Graham, A. 1988a. Studies in Neotropical paleobotany. V. The Lower Miocene communities of Panama—the Culebra Formation. Annals Missouri Botanical Garden 75:1440–1466.

Graham, A. 1988b. Studied in Neotropical paleobotany. VI. The Lower Miocene communities of Panama—the Cucaracha Formation. Annals Missouri Botanical Garden 75:1467–1479.

Graham, A. 1999a. Studies in Neotropical botany. XIII. An Oligo-Miocene palynoflora from Simojovel (Chiapas, Mexico). American Journal of Botany 86:17–31.

Graham, A. 1999b.The Tertiary history of the Northern Temperate Element in the Northern Latin American Biota. American Journal of Botany 86:32–38.

Hastings, A. K., J. I. Bloch, C. A. Jaramillo, A. F. Rincon, and B. J. MacFadden. 2013. Systematics and biogeography of crocodylians from the Miocene of Panama. Journal of Vertebrate Paleontology 33:239–263.

Head, J., A. F. Rincon, C. Suarez, C. Montes, and C. Jaramillo. 2012. Fossil evidence for earliest Neogene American faunal interchange: *Boa* (Serpentes, Boinae) from the early Miocene of Panama. Journal of Vertebrate Paleontology 32:1328–1334.

Herrera, F., S. Manchester, and C. Jaramillo. 2012. Permineralized fruits from the late Eocene of Panama give clues of the composition of forests established early in the uplift of Central America. Review of Palaeobotany and Palynology 175:10–24.

Illiger, C. 1811. Prodromus Systematis Mammalium et Avium Additis Terminis Zoographicis Utriusque Classis. C. Salfeld, Berlin, Germany, 301 pp.

Janis, C. M., J. Damuth, and J. M. Theodor. 2000. Miocene ungulates and terrestrial primary productivity: where have all the browsers gone? Proceedings of the National Academy of Sciences of the United States of America 97:237–261.

Jaramillo, C., E. Moreno, V. Ramirez, S. da Silva, A. Barrera, B. Adhara, S. Moron, F. Herrera, J. Escobar, J. R. Koll, S. Manchester, and N. Hoyos. 2014. Palynological record of the last 20 million years in Panama; pp. 134–253 in W. D. Stevens, O. M. Montiel, and P. H. Raven (eds.), Paleobotany and Biogeography: A Festschrift for Alan Graham in His 80th Year. Monographs in Systematic Botany 128, Missouri Botanical Garden Press, St. Louis.

Joeckel, R. M., and J. M. Stavas. 1996. Basicranial anatomy of *Syndyoceras cooki* (Artiodactyla, Protoceratidae) and the need for a reappraisal of tylopod relationships. Journal of Vertebrate Paleontology 16:320–327.

Jourdan, M. 1862. La description de restes fossils de grands mammifères. Part 2. Les terrains sidérolithiques. Revue des Sociétés Savantes 1:126–130.

Kirby, M. X., and B. J. MacFadden. 2005. Was southern Central America an archipelago or a peninsula in the middle Miocene? A test using land-mammal body size. Palaeogeography, Palaeoclimatology, Palaeoecology 228:193–202.

Kirby, M. X., D. S. Jones, and B. J. MacFadden. 2008. Lower Miocene stratigraphy along the Panama Canal and its bearing on the Central American peninsula. PLoS ONE 3:e2791. doi: 10.1371/journal.pone.0002791.

Linnaeus, C. 1758. Systema Naturae per Regna tria Naturae, secundum Classes, Ordines, Genera, Species, cum Characteribus, Differentis, Synonymis, Locis, 10th edition. Laurentius Salvius, Stockholm, Sweden, 824 pp.

Loomis, F. B. 1925. Dentition of artiodactyls. Proceedings of the Paleontological Society 36:583–604.

MacFadden, B. J. 2006. North American land mammals from Panama. Journal of Vertebrate Paleontology 26:720–734.

MacFadden, B. J. 2009. Three-toed browsing horse *Anchitherium* (Equidae) from the Miocene of Panama. Journal of Paleontology 83:489–492.

MacFadden, B. J., and P. Higgins. 2004. Ancient ecology of 15 million-year-old browsing mammals within C3 plant communities from Panama. Oecologia 140:169–182.

MacFadden, B. J., J. I. Bloch, H. Evans, D. A. Foster, G. S. Morgan, A. Rincon, and A. R. Wood. 2014. Temporal calibration and biochronology of the Centenario Fauna, Early Miocene of Panama. The Journal of Geology 122:113–135.

MacFadden, B. J., M. Kirby, A. Rincon, C. Montes, S. Moron, N. Strong, and C. Jaramillo. 2010. Extinct peccary "*Cynorca*" *occidentale* (Tayassuidae) from the Miocene of Panama and correlations to North America. Journal of Paleontology 84:288–298.

Maddison, W. P., and D. R. Maddison. 2009. Mesquite: A Modular System for Evolutionary Analysis, version 2.72. Available at http://mesquiteproject.org. Accessed December 2, 2010.

Maglio, V. J. 1966. A revision of the fossil selenodont artiodactyls from the middle Miocene Thomas Farm, Gilchrist County, Florida. Breviora 255:1–27.

Marsh, O. C. 1891. A horned artiodactyl (*Protoceras celer*) from the Miocene. The American Journal of Science and Arts (Series 3) 241:81–82.

Marsh, O. C. 1894. Description of Tertiary artiodactyls. American Journal of Science (Series 3) 48:259–274.

Marsh, O. C. 1897. Principal characters of the Protoceratidae. American Journal of Science (Series 4) 4:165–176.

Matthew, W. D. 1905. Notice of two new genera of mammals from the Oligocene of South Dakota. Bulletin of the American Museum of Natural History 21:21–26.

Montes, C., A. Cardona, R. McFadden, S. E. Moron, C. A. Silva, S. Restrepo-Moreno, D. A. Ramirez, N. Hoyos, J. Wilson, D. Farris, G. A. Bayona, C. A. Jaramillo, V. Valencia, J. Bryan, and J. A. Flores. 2012. Evidence for middle Eocene and younger emergence in Central Panama: implications for Isthmus closure. Geological Society of America Bulletin 124:780–799. doi: 10.1130/B30528.1.

Owen, R. 1848. Description of teeth and portions of two extinct anthracotheroid quadrapeds (*Hyopotamus vectianus* and *H. bovinus*) discovered by the Marchioness of Hastings in the Eocene deposits on the N. W. coast of the Isle of Wight, with an attempt to develop Cuvier's idea of the classification of pachyderms by the number of their toes. Quarterly Journal of the Geological Society of London 4:104–141.

Patton, T. H. 1969. Miocene and Pliocene artiodactyls, Texas Gulf Coastal Plain. Bulletin of the Florida State Museum, Biological Science 14:115–226.

Patton, T. H., and B. E. Taylor. 1971. The Synthetoceratinae (Mammalia, Tylopoda, Protoceratidae). Bulletin of the American Museum of Natural History 145:119–218.

Patton, T. H., and B. E. Taylor. 1973. The Protoceratinae (Mammalia, Tylopoda, Protoceratidae) and the systematics of the Protoceratidae. Bulletin of the American Museum of Natural History 150:347–414.

Peterson, O. A. 1931. New species from the Oligocene on the Uinta. Annals of the Carnegie Museum 21:61–78.

Prothero, D. R. 1998. Protoceratidae; pp. 431–438 in C. M. Janis, K. M. Scott, and L. L. Jacobs (eds.), Evolution of Tertiary Mammals of North America. Cambridge University Press, Cambridge, U.K., and New York.

Retallack, G. J., and M. Kirby. 2007. Middle Miocene global change and paleogeography of Panama. Palaios 22:667–669.

Rincon, A. F., J. I. Bloch, B. J. MacFadden, and C. A. Jaramillo. 2013. First Central American record of Anthracotheriidae (Mammalia, Bothriodontinae) from the early Miocene of Panama. Journal of Vertebrate Paleontology 33:421–433.

Rincon, A. F., J. I. Bloch, D. A. Foster, B. J. MacFadden, and C. A. Jaramillo. 2012a. The Las Cascadas fossil assemblage: biostratigraphic and paleobiogeographic implications of the oldest mammals from the Panama Canal area, Central America. Presented at the Geological Society of America Meeting, Charlotte, North Carolina, November 4–7, 2012. Paper No. 58–4. Geological Society of America abstracts with programs 44(7):163. Available at https://gsa.confex.com/gsa/2012AM/finalprogram/abstract_212288.htm. Accessed January 15, 2013.

Rincon, A. F., J. I. Bloch, B. J. MacFadden, C. Suarez, and C. A. Jaramillo. 2012b. New floridatragulines (Mammalia, Camelidae) from the early Miocene Las Cascadas Formation, Panama. Journal of Vertebrate Paleontology 32:456–475.

Rooney, T., P. Franceschi, and C. Hall. 2010. Water saturated magmas in the Panama Canal region: a precursor to Adakite-like magma generation. Contributions to Mineralogy and Petrology 161:373–388.

Scott, W. B. 1940. Artiodactyla; pp. 363–746 in W. B. Scott, and G. L. Jepsen (eds.), The Mammalian Fauna of the White River Oligocene. Transactions of the American Philosophical Society, Philadelphia 28(4):1–980.

Scott, W. B., and H. F. Osborn. 1887. Preliminary report on the vertebrate fossils of the Uinta Formation, collected by the Princeton Expedition of 1886. Proceedings of the American Philosophical Society 24:255–264.

Simpson, G. G. 1945. The principles of classification and a classification of mammals. Bulletin of the American Museum of Natural History 85:1–350.

Solórzano-Kraemer, M. M. 2007. Systematic, palaeoecology, and palaeobiogeography of the insect fauna from Mexican amber. Palaeontographica A 282:1–133.

Solórzano-Kraemer, M. M. 2010. Mexican amber; pp. 42–56 in D. Penney (ed.), Biodiversity of Fossils in Amber from Major World Deposits. Siri Scientific Press, Manchester, U.K.

Stirton, R. A. 1944. Comments on the relationship of the cervoid family Palaeomerycidae. American Journal of Science 242:633–655.

Stirton, R. A. 1967. Relationships of the Protoceratid Artiodactyls and Description of a New Genus. University of California Press, Berkeley, California, 44 pp.

Strömberg, C. A. E. 2002. The origin and spread of grass-dominated ecosystems in the Late Tertiary of North America: preliminary results concerning the evolution of hypsodonty. Palaeogeography, Palaeoclimatology, Palaeoecology 177:59–75.

Strömberg, C. A. E. 2006. Evolution of hypsodonty in equids: testing a hypothesis of adaptation. Paleobiology 32:236–258.

Swofford, D. A. 2003. PAUP*: Phylogenetic Analysis Using Parsimony (and Other Methods), version 4.0. Sinauer Associates, Sunderland, Massachusetts.

Tedford, R. H. 1970. Principles and practices of mammalian geochronology in North America; pp. 666–703 in Field Museum of Natural History (ed.), Proceedings of the North American Paleontological Convention September 5–7, 1969, Part F: Correlation by fossils. Allen Press, Chicago.

Tedford, R. H., and M. E. Hunter. 1984. Miocene marine-nonmarine correlations, Atlantic and Gulf Coastal Plains, North America. Paleogeography, Paleoclimatology, Paleoecology 47:129–152.

Tedford, R. H., L. B. Albright III, A. D. Barnosky, I. Ferrusquia-Villafranca, R. M. Hunt Jr., J. E. Storer, C. C. Swisher III, M. R. Voorhies, S. D. Webb, and D. P. Whistler. 2004. Mammalian biochronology of the Arikareean through Hemphillian interval (late Oligocene through early Pliocene epochs); pp. 169–231 in M. O. Woodburne (ed.), Late Cretaceous and Cenozoic Mammals of North America: Biostratigraphy and Geochronology. Columbia University Press, New York.

Troxell, E. L. 1921. A study of *Diceratherium* and the diceratheres. American Journal of Science (Series 5) 2:197–208.

Vega, F. J., T. Nyborg, M. A. Coutiño, J. Solé, O. Hernández-Monzón. 2009. Neogene Crustacea from Southeastern Mexico. Bulletin of the Mizunami Fossil Museum, 35:51–69.

Webb, S. D. 1981. *Kyptoceras amatorum*, a new genus and species from the Pliocene of Florida, the last protoceratid artiodactyl. Journal of Vertebrate Paleontology 1:357–365.

Webb, S. D., and B. E. Taylor. 1980. The phylogeny of hornless ruminants and a description of the cranium of *Archaeomeryx*. Bulletin of the American Museum of Natural History 167: 121–157.

Webb, S. D., B. L. Beatty, and G. Poinar Jr. 2003. New evidence of Miocene Protoceratidae including a new species from Chiapas, Mexico. Bulletin of the American Museum of Natural History 279:348–367.

Whitmore, F. C., and R. H. Stewart. 1965. Miocene mammals and Central American seaways. Science 148:180–185.

Wilson, J. A. 1974. Early Tertiary vertebrate faunas, Vieja Group and Buck Hill Group, trans-Pecos Texas: Protoceratidae, Camelidae, Hypertragulidae. Texas Memorial Museum, Bulletin 23:1–34.

Wood, H. E., II. 1964. Rhinoceroses from the Thomas Farm Miocene of Florida. Museum of Comparative Zoology Bulletin 130:361–386.

Woodburne, M. O. 1969. Systematics, biogeography, and evolution of *Cynorca* and *Dyseohyus* (Tayassuidae). Bulletin of the American Museum of Natural History, 141:271–356.

Woodburne, M. O. 2004. Principles and procedures; pp. 1–20 in M. O. Woodburne (ed.), Late Cretaceous and Cenozoic Mammals of North America: Biostratigraphy and Geochronology. Columbia University Press, New York.

Woodburne, M. O. 2010. The Great American Biotic Interchange: dispersals, tectonics, climate, sea level and holding pens. Journal of Mammalian Evolution 17:245–264.

Woodring, W. P. 1957. Geology and paleontology of Canal Zone and adjoining parts of Panama; description of Tertiary mollusks; gastropods; Trochidae to Turritellidae. U.S. Geological Survey Professional Paper 306-A:1–239.

Woodring, W. P. 1982. Geology and paleontology of Canal Zone and adjoining parts of Panama; description of Tertiary mollusks; pelecypods, Propeamussiidae to Cuspidariidae; additions to families covered in P306-E; additions to gastropods; cephalopods. U.S. Geological Survey Professional Paper 306–7:541–759.

Woodring, W. P., and T. F. Thompson. 1949. Tertiary formations of Panama Canal Zone and adjoining parts of Panama. American Association of Petroleum Geologists Bulletin 33:223–247.

Wortman, J. L. 1898. The extinct Camelidae of North America and some associated forms. Bulletin of the American Museum of Natural History 10:93–142.

Submitted October 7, 2013; revisions received September 3, 2014;
accepted September 9, 2014.
Handling editor: Thomas Martin.

Citation for this article: Rincon, A. F., J. I. Bloch, B. J. Macfadden, and C. A. Jaramillo. 2015. New early Miocene protoceratids (Mammalia, Artiodactyla) from Panama. Journal of Vertebrate Paleontology. DOI: 10.1080/02724634.2015.970688.

APPENDIX 1. Dental measurements of *Paratoceras* from the early Miocene of Panama. **Abbreviations: APL**, anterior-posterior length; **TWHyd**, transverse hypoconulid width; **TWmx**, maximum transverse width. *Highly deformed fossils excluded from the statistical summary.

Taxon	UFcatalog number	Tooth position	APL (mm)	TWmx (mm)	TWHyd (mm)
P. coatesi	UF 271182	Rp1	6.36	3.55	—
P. coatesi	UF 271623	Lp1	6.26	3.62	—
P. coatesi	UF 271181	Rp2	13.74	6.10	—
P. coatesi	UF 267123*	Lp2	14.31	5.76	—
P. coatesi	UF 271182	Rp3	13.99	6.29	—
P. coatesi	UF 271624*	Rp3	15.50	6.03	—
P. coatesi	UF 223328*	Rp3	12.30	5.25	—
P. coatesi	UF 271181	Rp3	13.48	6.45	—
P. coatesi	UF 280222	Rp3	12.47	6.17	—
P. coatesi	UF 271623	Lp3	13.36	6.31	—
P. coatesi	UF 267123*	Lp3	16.27	7.43	—
P. coatesi	UF 271182	Rp4	10.76	7.43	—
P. coatesi	UF 271624*	Rp4	11.67	7.45	—
P. coatesi	UF 223328*	Rp4	9.90	6.50	—
P. coatesi	UF 271181	Rp4	10.67	7.93	—
P. coatesi	UF 280222	Rp4	8.95	7.34	—
P. coatesi	UF 223094	Lp4	9.96	7.56	—
P. coatesi	UF 271623	Lp4	10.56	7.76	—
P. coatesi	UF 267124*	Lp4	11.17	8.14	—
P. coatesi	UF 267123*	Lp4	13.68	9.63	—
P. coatesi	UF 267125	Lp4	10.66	7.72	—
P. coatesi	UF 280222	Rm1	11.66	10.60	—
P. coatesi	UF 271182	Rm1	11.90	10.96	—
P. coatesi	UF 271624*	Rm1	14.13	10.50	—
P. coatesi	UF 223328*	Rm1	10.26	8.81	—
P. coatesi	UF 271181	Rm1	12.01	11.69	—
P. coatesi	UF 271623	Lm1	11.55	9.66	—
P. coatesi	UF 237854	Lm1	11.85	9.90	—
P. coatesi	UF 223094	Lm1	12.21	10.61	—
P. coatesi	UF 267124*	Lm1	12.29	11.47	—
P. coatesi	UF 267123*	Lm1	12.66	12.39	—
P. coatesi	UF 236927	Lm1	11.66	10.01	—
P. coatesi	UF 280222	Rm2	12.36	12.02	—
P. coatesi	UF 271182	Rm2	13.18	11.73	—
P. coatesi	UF 271624*	Rm2	16.35	11.93	—
P. coatesi	UF 271181	Rm2	13.22	13.39	—
P. coatesi	UF 223328*	Rm2	12.77	9.92	—
P. coatesi	UF 271623	Lm2	13.15	11.80	—
P. coatesi	UF 237854	Lm2	13.71	12.63	—
P. coatesi	UF 223094	Lm2	14.54	12.72	—
P. coatesi	UF 267124*	Lm2	12.43	12.98	—
P. coatesi	UF 267123*	Lm2	14.33	12.50	—
P. coatesi	UF 271182	Rm3	17.98	11.52	6.89
P. coatesi	UF 271624*	Rm3	19.22	12.53	6.77
P. coatesi	UF 223328*	Rm3	19.70	9.90	6.84
P. coatesi	UF 271596	Rm3	17.99	11.23	6.53
P. coatesi	UF 271623	Lm3	18.12	10.95	6.91
P. coatesi	UF 237854	Lm3	20.62	11.82	7.01
P. coatesi	UF 223094	Lm3	17.92	12.72	7.15
P. coatesi	UF 267124*	Lm3	16.18	12.67	6.70
P. coatesi	UF 267123*	Lm3	21.75	13.01	6.90
P. coatesi	UF 271150	Lm3	17.38	12.03	7.10
P. orarius	UF 237878	Lm1	9.25	7.18	—
P. orarius	UF 237878	Lm2	10.42	8.01	—
P. orarius	UF 237878	Lm3	13.95	8.18	4.98
P. orarius	UF 271625	Rp3	10.73	4.27	—
P. orarius	UF 271625	Rp4	8.45	5.37	—
P. orarius	UF 271625	Rm1	9.42	7.61	—
P. orarius	UF 271625	Rm2	10.05	8.40	—
P. orarius	UF 271625	Rm3	15.36	8.43	—
P. orarius	UF 280222	Rm2	9.84	7.62	—
P. orarius	UF 280223	Lm2	9.70	7.84	—
P. aff. *tedfordi*	UF 254121	Lm2	12.97	10.20	—
P. aff. *tedfordi*	UF 271179	Lm2	13.51	10.32	—
P. aff. *tedfordi*	UF 254119	Rp4	10.54	6.50	—
P. aff. *tedfordi*	UF 271622	Lm2	14.60	10.66	—
P. aff. *tedfordi*	UF 271627	Rm2	13.88	10.77	—
P. aff. *tedfordi*	UF 267194	Rp4	11.60	7.01	—
P. aff. *tedfordi*	UF 267194	Rm1	10.55	9.24	—
P. aff. *tedfordi*	UF 267194	Rm2	12.12	11.27	—

(*Continued on next page*)

APPENDIX 1. Dental measurements of *Paratoceras* from the early Miocene of Panama. **Abbreviations: APL**, anterior-posterior length; **TWHyd**, transverse hypoconulid width; **TWmx**, maximum transverse width. *Highly deformed fossils excluded from the statistical summary (*Continued*)

Taxon	UFcatalog number	Tooth position	APL (mm)	TWmx (mm)	TWHyd (mm)
P. aff. *tedfordi*	UF 267194	Rm3	18.12	10.67	6.85
P. aff. *tedfordi*	UF 275168	Lm2	13.84	10.11	—
P. aff. *tedfordi*	UF 275168	Lm3	21.08	10.40	6.56
P. aff. *tedfordi*	UF 241199	LP2	12.22	8.70	—
P. aff. *tedfordi*	UF 271626	RP3	10.41	5.97	—
P. aff. *tedfordi*	UF 236931	LM2	13.03	16.68	—
P. aff. *tedfordi*	UF 271618	RP4	8.78	11.01	—
P. coatesi	UF 237877	RP2	12.63	6.18	—
P. coatesi	UF 237877	RP3	12.65	8.58	—
P. coatesi	UF 223584	LP3	11.79	8.46	—
P. coatesi	UF 236913	RP4	8.22	13.47	—
P. coatesi	UF 237877	RP4	9.41	12.30	—
P. coatesi	UF 223585	RP4	8.83	13.83	—
P. coatesi	UF 223584	LP4	7.79	11.53	—
P. coatesi	UF 236913	RM1	11.06	14.48	—
P. coatesi	UF 223585	RM1	10.81	14.80	—
P. coatesi	UF 237862	LM1	11.29	14.34	—
P. coatesi	UF 223326	LM1	11.37	15.73	—
P. coatesi	UF 223584	LM1	10.99	13.49	—
P. coatesi	UF 223585	LM1	11.04	15.03	—
P. coatesi	UF 237877	RM2	12.83	16.44	—
P. coatesi	UF 223585	RM2	12.92	17.77	—
P. coatesi	UF 223326	LM2	11.92	17.16	—
P. coatesi	UF 223585	LM2	12.82	17.94	—
P. coatesi	UF 236917	RM3	13.36	17.65	—
P. coatesi	UF 237877	RM3	11.79	16.08	—
P. coatesi	UF 223585	RM3	12.26	17.21	—
P. coatesi	UF 223326	LM3	11.63	16.18	—
P. coatesi	UF 280221	RM3	13.58	16.18	—
P. coatesi	UF 223585	LM3	12.43	16.91	—
P. coatesi	UF 275284	RM3	13.30	17.80	—

APPENDIX 2. Description of dental and cranial characters used in the phylogenetic analysis. All characters are treated as unordered.

(1) Anterior end of nasal bones: anterior to P3 (0); posterior to P3 (1).
(2) Upper molars: square, brachydont, with thick enamel APL/TW ratio >0.8 (0); wider than longer, brachydont, with thick enamel, APL/TW ratio <0.8 (1).
(3) Protocone on upper P3: strongly developed forming an internal cusp lingual to the paracone (0); reduced and restricted to the basal part of the crown (1); reduced to basal cingular segments interrupted by an inflate paracone (2); absent (3).
(4) Cinguli on upper molars: discontinuous, strong and tall forming a shelf between protocone and metaconule (0); strong and restricted to the anterior part of the protocone and metaconule (1); strong and basal but continuous (2).
(5) Horizontal lateral ridge extending from the outer face of the maxillary bone to the orbit: weak or absent (0); strong and continuous (1); strong and discontinuous (2).
(6) Anterior end of the orbits: posterior to M3 (0); anterior to M3 (1).
(7) Protoconid on p4: strong with a tall metaconid running lingually, entoconid weak and low (0); reduced forming an open valley with the hypoconid, no entoconid (1); reduced but forming a narrow valley with the hypoconulid (2).
(8) p4 morphology: APL/TW ratio: elongated, ratio >1.6 (0); shortened ratio <1.6 (1).
(9) Parastylid on lower molars: strong (0); weak or absent (1).
(10) APL m1/p4: <1.0 (0); >1.0 (1).
(11) Strong protocone on P2: present (0); absent (1).
(12) Morphology of the labial margin of P3: labially concave (0); straight with reduced parastyle (1).
(13) p4 talonid morphology: elongated, entoconid entostylid slightly divergent, deep fossetid (0); reduced, entoconid entostilid divergent, deep fossetid (1); anterioposteriorly reduced forming a wedge-shaped tooth with a bulbous talonid and shallow fossetid (2).
(14) p3 hypoconid reaching the protoconid (0); p3 hypoconid reaching the metaconid (1).
(15) Paraconid on p3: absent (0); present and lingually inflected (1); enlarged or bulbous (2).

APPENDIX 3. Character-taxon matrix used in phylogenetic analysis of 'Protoceratinae.' See Appendix 2 for character descriptions.

	1234567890	*112345*
Heteromeryx dispar	*0010000001?*	*000?0*
Pseudoprotoceras longinaris	*0012?000??*	*10???*
Pseudoprotoceras taylori	*0030000???*	*11???*
Protoceras neatodelpha	*?0111?1???*	*10?0?*
Protoceras celer	*0001101010*	*00101*
Paratoceras tedfordi	*1022?1????*	*?1???*
Paratoceras aff. tedfordi	*?122??1000*	*111??*
Paratoceras orarius	*??????2111*	*?1211*
Paratoceras wardi	*1122112101*	*11111*
Paratoceras macadamsi	*???????2111*	*11212*
Paratoceras coatesi	*1122112111*	*11211*